Landscape Ecol (2020) 35:293–318
https://doi.org/10.1007/s10980-019-00947-z

RESEARCH ARTICLE

Multi-scaled drivers of severity patterns vary across land ownerships for the 2013 Rim Fire, California

Nicholas A. Povak · Van R. Kane · Brandon M. Collins · Jamie M. Lydersen · Jonathan T. Kane

Received: 28 January 2019 / Accepted: 28 November 2019 / Published online: 20 December 2019
© This is a U.S. government work and its text is not subject to copyright protection in the United States; however, its text may be subject to foreign copyright protection 2019

Abstract

Context As the frequency of large, severe fires increases, detecting the drivers of spatial fire severity patterns is key to predicting controls provided by weather, fuels, topography, and management.

Objectives Identify the biophysical and management drivers of severity patterns and their spatial variability across the 2013 Rim Fire, Sierra Nevada, California, USA.

Methods Random forest models were developed separately for reburned and fire-excluded (> 80 year) areas within Yosemite National Park (NP) and Stanislaus National Forest (NF). Models included biophysical, past disturbance, and spatial autocorrelation (SA) predictors. Variable importance was assessed globally and locally. Variance partitioning was used to assess pure and shared variance among predictors.

Results High spatial variability in the relative dominance of predictors existed across burn days and between land ownerships. Fire weather was a dominant top-down control during plume-dominated fire spread days. However, bottom-up controls from fuels and topography created local, fine-scale heterogeneity throughout. Reburn severity correlated with previous severity suggesting strong landscape memory, particularly in Yosemite NP. SA analysis showed broad-scale spatial dependencies and high shared variance among predictors.

Conclusions Wildfires are inherently a multi-scaled process. Spatial structure in environmental variables

Electronic supplementary material The online version of this article (https://doi.org/10.1007/s10980-019-00947-z) contains supplementary material, which is available to authorized users.

N. A. Povak
USDA Forest Service, Pacific Northwest Research Station, Wenatchee Forestry Sciences Lab, Wenatchee, WA 98801, USA

N. A. Povak (✉)
Oak Ridge Institute for Science and Education (ORISE), Oak Ridge, TN 37830, USA
e-mail: nicholas.povak@usda.gov

V. R. Kane · J. T. Kane
School of Environmental and Forest Sciences, University of Washington, Box 352100, Seattle, WA 98195, USA

B. M. Collins
Center for Fire Research and Outreach, University of California, Berkeley, CA 94720, USA

J. M. Lydersen
Department of Environmental Science, Policy and Management, University of California, Berkeley, CA 94720, USA

Present Address:
J. M. Lydersen
California Department of Forestry and Fire Protection, Fire and Resource Assessment Program, Sacramento, CA 95818, USA

create broad-scale patterns and dependencies among drivers leading to regions of similar fire behavior, while local bottom-up drivers generate fine-scaled heterogeneity. Identifying the conditions under which top-down factors overwhelm bottom-up controls can help managers monitor and manage wildfires to achieve both suppression and restoration goals. Restoration targeting both surface and ladder fuels can mediate future fire severity even under extreme weather conditions.

Keywords Fire severity · Machine learning · Variable importance · Spatial autocorrelation · Variance partitioning · Rim fire

Introduction

Changing fire regimes in some forests resulting from ongoing climate change and past management practices have altered the role of wildfire in fire-dependent systems (Heyerdahl et al. 2001; Hessburg and Agee 2003; Lydersen and Collins 2018; Hessburg et al. 2019). Forests in the western U.S. historically characterized by frequent, mixed-severity fire regimes experienced an extended period of fire exclusion over the past century due to effective fire suppression policies and mild climate conditions. This resulted in increased stand density driven by shade tolerant trees (Hessburg et al. 2005; Scholl and Taylor 2010; Collins et al. 2011; Lydersen and Collins 2018). Changes in vegetation and fuel structure, coupled with changes in climate, have contributed to considerable increases in annual area burned (Dennison et al. 2014; Westerling 2016) and the size and dominance of stand-replacing fire patches (Miller and Safford 2012; Cansler and McKenzie 2014; Stevens et al. 2017; Singleton et al. 2019).

The increasing incidence of very large wildfires (> 10,000 ha) has led to substantive changes in the size distribution of wildfires (Cui and Perera 2008; Dennison et al. 2014; Barbero et al. 2015). This trend has spurred an interest in the underlying relationships between burn patterns and the drivers of fire size and severity. Large fire events often coincide with extreme weather resulting in severe fire effects (Peterson et al. 2015; Coen et al. 2018; Lareau et al. 2018) that can negatively impact short- and long-term ecological processes (Stephens et al. 2014). However, in some areas, large fires were common historically and can currently provide important ecological benefits (Bradstock 2009; Hammill and Bradstock 2009; Keane et al. 2009). Large fire frequency is expected to increase under climate change (Stavros et al. 2014), and information gaps exist regarding their ecological causes, consequences, and management implications. Investigations into the drivers of large fire severity patterns, their landscape variability, and potential thresholds where top-down factors exceed the capacity for finer-scale patterns to affect fire behavior are critical research topics (Finney 2001; O'Connor et al. 2017).

Correlative modeling and spatial autocorrelation

Remotely-sensed data are commonly used to study the drivers of fire severity patterns across large landscapes (Prichard and Kennedy 2014; Kane et al. 2015a; Parks et al. 2018b). Fire severity is defined as the amount of fire-related change to ecosystem components such as soil and vegetation (Key and Benson 2006; Parks et al. 2018b). Fire severity indices are developed from detected changes in soil and vegetation reflectance and statistically related to biophysical and disturbance history variables, which influence these patterns. Variability in fire weather, fuels, and topography across the landscape manifests in heterogeneous burn patterns as their influence and interdependence change, often in complex ways, within and among fires, which creates challenges for traditional statistical models (Bradstock et al. 2010; Parks et al. 2011).

Machine learning models have been incorporated into ecological research to infer complex statistical relationships and interactions between ecological patterns and processes (Elith et al. 2006; Cutler et al. 2007; Olden et al. 2008). These models produce accurate predictions while still exposing model behavior and assessing model errors similar to more traditional linear models. However, these models must also account for the inherent spatial autocorrelation (SA) associated with environmental patterns and the contagious nature of fire spread (Wimberly et al. 2009; Prichard and Kennedy 2014; Portier et al. 2018). SA describes the similarities in observations related to their geographic distance (Legendre 1993). In parametric regression, SA invalidates the assumption of model residuals being independent and identically distributed. Strong SA can lead to selection of weak

predictors and makes inferences of model results to other geographies difficult (Legendre 1993; Dormann et al. 2007; Hawkins et al. 2007). Less is known about the effects of SA in machine learning, however, recent research has shown increased model accuracy and reduced SA in model residuals when methods to account for SA are used (e.g., Crase et al. 2012; Václavík et al. 2012; Mascaro et al. 2014; Ryo et al. 2018; Portier et al. 2018).

Methods for controlling SA in fire severity modeling have varied. Gridded sampling uses a minimum sampling distance to reduce the spatial dependence among sample points (Odion et al. 2004; Parks et al. 2014; Birch et al. 2015; Kane et al. 2015a). Alternatively, Wimberly et al. (2009) and Prichard and Kennedy (2014) used sequential autoregression (SAR) to model the effects of fuels-reduction treatments on fire severity patterns. SAR incorporated SA by including information on the severity of neighboring grid cells into a spatially explicit term in the linear model. Models had high accuracy in predicting fire severity patterns and confidence in identifying treatment effects on mitigating fire severity. Portier et al. (2018) used residuals autocovariate (RAC) models to predict burn rates in coniferous boreal forests of eastern Canada. These models derived a spatially-explicit covariate from the residuals of an initial environment-only model, and the authors found higher model performance for RAC models compared to the environment-only models.

Within fire modeling, SA modeling methods have not yet been incorporated into a machine learning context, and an explicit estimation of the scale and overall influence of SA on model results is still lacking. Furthermore, the methods outlined above do not quantify the variability in fire severity that is attributable to SA alone or jointly with other predictor variables, although current methods could be extended to achieve this goal.

Study objectives

We applied a machine learning framework to assess the main environmental drivers, their spatial structure, and variability for the 2013 Rim Fire located in the Sierra Nevada Mountains of California, USA. The Rim Fire burned more than 100,000 ha within the Stanislaus National Forest (NF) and Yosemite National Park (NP) in California, USA, making it one of the five largest fires in California history to date. The fire burned across a variety of biophysical conditions and vegetation types, experienced several plume-dominated fire days leading to rapid fire growth, and spanned a variety of land ownerships that experienced different forest management and fire histories (Collins et al. 2017a).

The spatial drivers of Rim Fire severity have previously been studied with a wide range of objectives (Lydersen et al. 2014; Harris and Taylor 2015; Kane et al. 2015a; Harris and Taylor 2017; Lydersen et al. 2017). Kane et al. (2015a) focused on reburned patches for a small portion of the Rim Fire footprint within Yosemite NP where LiDAR data were acquired and used machine learning models to relate a variety of climate, weather, fire history, and forest structure variables to severity. Harris and Taylor (2017) focused on reburns throughout the fire and modeled the relationships among biophysical and fire history predictors. Lydersen et al. (2017) investigated the drivers of Rim Fire severity within reburns and previously managed treatment units.

Our study complements this previous work by providing a comprehensive assessment of the drivers of fire severity across the entire burned area. We include an examination of the spatial trends in local variable importance to assess changes in the relative influence of variables across heterogeneous environments and burn days. We also incorporate an explicit analysis on the effects of spatial autocorrelation on fire severity patterns, which is often missing from studies of large wildfires.

We addressed the following research questions:

1. How did the importance of top-down and bottom-up drivers vary spatially?
2. Were differences in managed (Stanislaus NF) and unmanaged (Yosemite NP) landscapes reflected in the main drivers of fire severity patterns?
3. Under what conditions do past management units influence subsequent fire effects?
4. What is the role of SA in modeling fire severity patterns using machine learning?

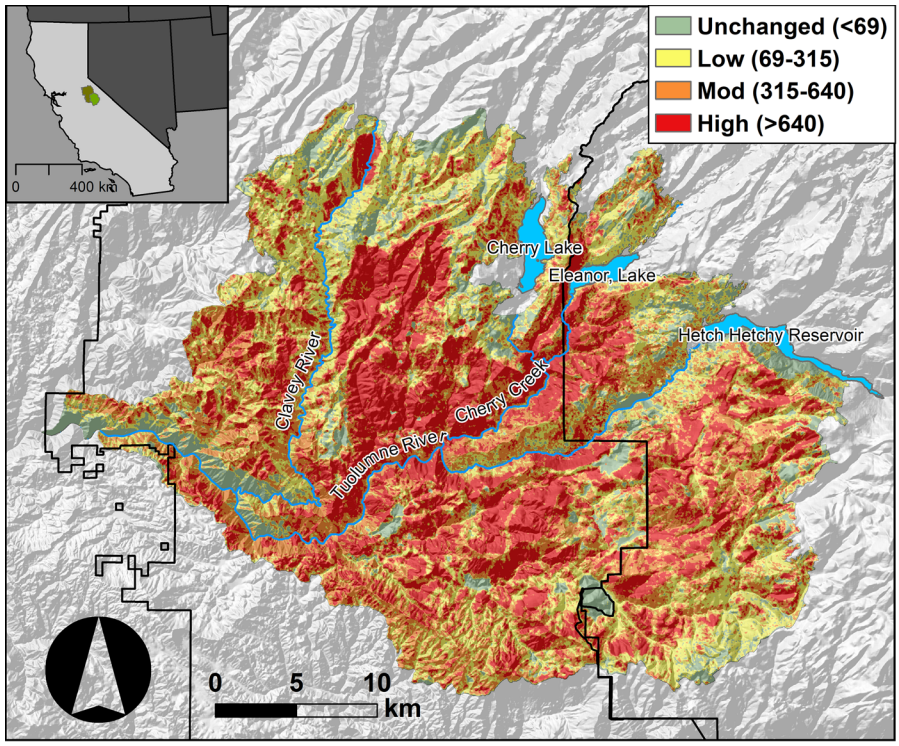

Fig. 1 Location map for the 2013 Rim Fire. Black lines depict the Stanislaus National Forest (NF, west) and Yosemite National Park (NP, east) boundaries. The color gradient represents fire severity classes and associated RdNBR (relative differenced normalized burn ratio, 30 m resolution) cutoff values. The inset map in the topleft shows the location of Stanislaus NF (dark green) and Yosemite NP (light green). (Color figure online)

Methods

Study area

The Rim Fire was human ignited and burned 104,131 ha between August 17 and October 24, 2013 in the central Sierra Nevada (Fig. 1) during the second year of a major four-year drought. The fire started on the Stanislaus NF and spread east into Yosemite NP. Approximately 35% of the fire's area burned over 2 days (August 21 & 22), when plume-dominated, extreme fire behavior resulted from pyro-cumulonimbus formations under an unstable air mass (Fig. 2). In total, plume-dominated conditions existed over seven burn days covering 64% of the total burned area (Peterson et al. 2015).

The climate of the central Sierra Mountains in California is characterized as Mediterranean with cool winters and warm summers with most precipitation occurring in the winter. Prior to the Rim Fire, conifer forests were the dominant vegetation type (71%) followed by oak woodland (12%), shrubland (11%) and grassland (5%; LANDFIRE 2012).

The area burned in the Rim Fire had 60.1% within the Stanislaus NF, 30.7% in Yosemite NP, 8.9% in private land ownership, and $< 1\%$ in other Federal and county lands. Stanislaus NF has a long history of mining, homesteading, ranching and timber harvesting. Recently, thinning and fuels reduction treatments have been conducted to reduce fuel loads. In Yosemite NP, mechanical fuel management activities are rarely used, although a small portion of the park was logged in the early 20th century. Our analyses focused on both NF and NP lands as they represent $> 90\%$ of the total area burned by the Rim Fire, and allowed for a comparison in severity patterns across differing management objectives regarding harvesting, fire suppression and prescribed burning practices (Johnson et al. 2013). However, differences also exist in the biophysical setting (Table 1) and dominant vegetation types

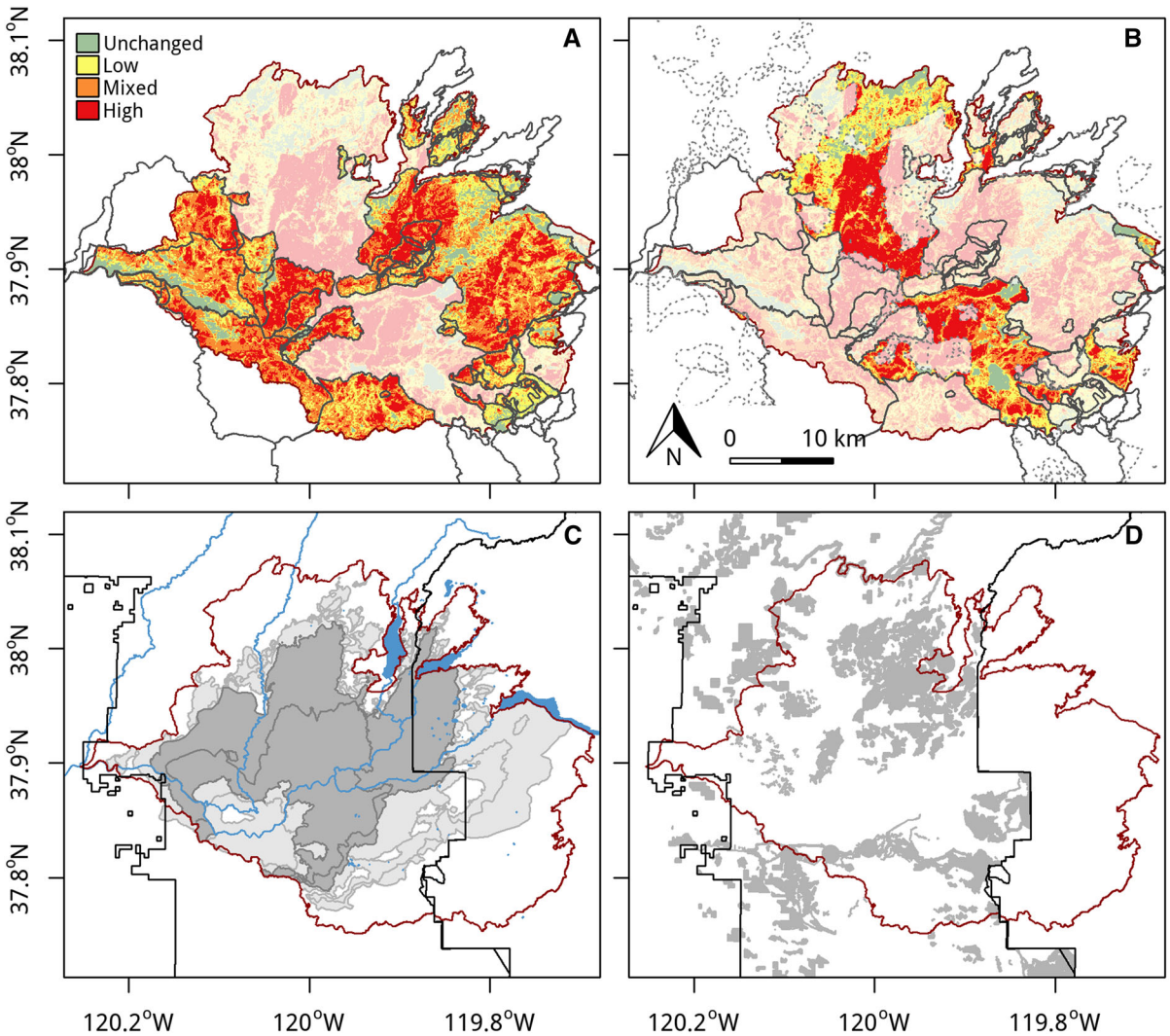

Fig. 2 Rim fire severity (RdNBR, 30 m resolution) for areas that **a** burned between 1984 and 2012 (i.e., reburns), and **b** for areas that had not burned since at least 1930 (i.e., first-entry fires). Dark grey lines represent fires that burned between 1984–2012, and light grey dotted lines represent fires that burned between 1908–1983. **c** Plume-dominated Rim fire progression days. Dark grey polygons represent the top two ranked burn days by area burned (August 21 & 22), while the light grey depict the remaining days with plume-dominanted fire behavior. Major streams and lakes are included for reference. **d** Management units (1995–2012) where mechanical thinning or other even- and unevenaged-management activities were conducted, and/or where mechanical surface treatments were used to reduce fuel loads. Black lines in panels C and D represent the boundaries of Stanislaus NF and Yosemite NP

(Table 2) between the two land designations. Namely, the Rim Fire in Yosemite NP burned at higher elevation, and included a larger proportion of red fir-dominated forests, which historically had longer fire return intervals (Beaty and Taylor 2001). Stanislaus NF included a higher proportion of mixed oak woodland and mixed conifer forest (Table 2).

Fire severity data

Following Lydersen et al. (2016), we used relative differenced Normalized Burn Ratio rasters based on 1-year post-fire assessment (RdNBR, 30-m resolution) to quantify fire severity patterns across the Rim Fire and all previous fires that burned within its extent (≥ 80-ha, 1984–2012) (Miller et al. 2009; Miller and

Table 1 Fifth, fiftieth, and ninety-fifth percentile values across 30 m pixels for elevation, climate normals, annual climate variability and daily fire weather variables for the 2013 Rim Fire burned area within the Stanislaus NF and Yosemite NP

Variable	Temporal resolution	Spatial resolution	Units	Stanislaus NF			Yosemite NP		
				5th	50th	95th	5th	50th	95th
Elevation	N/A	10-m	m	668.2	1270.7	1767.0	1309.6	1759.6	2176.4
Actual evapotranspiration	30-year normal	270-m	mm	345.0	425.4	538.8	258.0	380.5	446.0
Water deficit	30-year normal	270-m	mm	508.9	683.5	797.9	464	560.9	718.0
Precipitation	30-year normal	270-m	mm	892.6	1047.0	1207.3	951.4	1088.1	1270.3
April snow pack	30-year normal	270-m	mm	0.0	8.0	224.2	15.3	123.1	374.0
Maximum temperature	Annual (2013)	270-m	%	46.5	66.7	84.1	46.4	75.0	93.1
Precipitation	Annual (2013)	270-m	%	14.8	24.9	34.1	15.9	24.9	36.4
Snow pack	Annual (2013)	270-m	%	44.3	76.0	88.6	46.9	68.1	82.1
Energy release component	Daily	4-km	Unitless	64.4	78.8	81.3	68.1	72.1	79.1
Burning index	Daily	4-km	Unitless	48.9	55.9	73.0	51.0	57.2	73.1

Table 2 Percent composition of dominant 2012 LANDFIRE Enhanced Vegetation Type classes across the Stanislaus NF and Yosemite NP land designations within the footprint of the 2013 Rim Fire

EVT class	ID	Stanislaus NF	Yosemite NP
Mediterranean california mesic mixed conifer forest and woodland	3028	30.9	42.6
Mediterranean california mixed oak woodland	3029	19.8	6.4
Mediterranean california red fir forest	3032	1.4	20.1
Mediterranean california dry-mesic mixed conifer forest and woodland	3027	14.6	5.2
California montane woodland and chaparral	3098	5.5	6.1
Mediterranean california lower montane conifer forest and woodland	3030	6.5	1.3
California montane riparian systems	3152	3.2	4.1
California lower montane foothill pine woodland and savanna	3114	6.7	0.2
California montane jeffrey pine (-ponderosa pine) woodland	3031	4.7	2.2
Mediterranean california sparsely vegetated systems II	3221	1.4	3.6
North pacific montane grassland	3138	1.3	2.5
Northern and central california dry-mesic chaparral	3105	1.1	0.2

Classes included in the table represent those that accounted for $> 1\%$ coverage for both areas and represent 97 and 95% of the Rim Fire area within Stanislaus NF and Yosemite NP, respectively

Quayle 2015; Lydersen et al. 2016). RdNBR is a satellite-derived measure of the loss of photosynthetic materials following a fire and is a surrogate for quantifying fire effects on ecosystem change (Table S1). Large values indicate large decreases in photosynthetic materials and surface materials holding water and an increase in ash, carbon, and exposed soil (Miller and Thode 2007). Miller et al. (2009) showed positive non-linear relationships between RdNBR and a series of forest plot-based estimates of fire-caused vegetation loss in the Sierras. Data were retrieved from a database maintained by the US Forest Service, Pacific Southwest Region. An additional dataset developed by Lutz et al. (2011) was used to extend the lower size threshold to fires $\geq$ 40 ha (1984–2010) within Yosemite NP. The dataset included a total of 49 fires that burned from 1984–2012 and ranged in size from 4 to 24,000 ha.

We were interested in modeling both fire-excluded and reburned areas (Fig. 2). The former had no record

of burning since 1930 (van Wagtendonk 2012), while the latter burned between 1984 and 2012 and included fire severity data. In total, we developed four RF models: (1) Stanislaus NF, reburned areas; (2) Stanislaus NF, fire-excluded areas; (3) Yosemite NP, reburned areas; and (4) Yosemite NP, fire-excluded areas.

Predictor variables

Table 3 includes a description of the predictor variables. Native raster resolution varied from 10 to 4,000-m across predictor variables (Table 3). All rasters were resampled to 30-m resolution to match the RdNBR data.

Fire history

Fire perimeter data (1930–2013) were downloaded from the California FRAP (Fire and Resource Assessment Program) database and were used to remove areas that experienced fire but did not include severity data.

For reburn models, predictor variables included: the number of past fires, years since last fire, maximum previous RdNBR (Kane et al. 2015b; Lydersen et al. 2017), and the distance from past fire boundary. The latter only included fires that burned < 10 years prior to the Rim Fire, which corresponds to a threshold where past fires provide limited control on subsequent fires (Collins et al. 2009). Values for this variable were negative for pixels within the perimeter of a previous fire, and positive for pixels outside previous fires.

Climate and climate variablity

To quantify spatial variability in long-term climate, we used 30-year climate normals data from the 2014 California Basin Characterization Model (BCM, http://climate.calcommons.org) (Flint et al. 2013). BCM uses a gradient-inverse distance squared approach to spatially downscale PRISM climate data (PRISM Climate Group 2013) from 800 to 270 m. We used climate normals data calculated for the years 1981–2010 to represent long-term actual evapotranspiration (AET), climatic water deficit, maximum temperature, annual precipitation, and April 1 snowpack (Tables 1, 3).

The BCM dataset was also used to represent percentile conditions for the year of the Rim Fire (2013, lag0) and year prior to fire (2012, lag1) for the same set of predictor variables. Annual data were downloaded for the years 1969–2013 in their native units from which percentiles were calculated for each pixel (Tables 1, 3).

Fire weather

To characterize local weather conditions for each daily burn period, we used the spatially explicit 4-km GRIDMET daily weather from Abatzaglou et al. (2013). While these data are coarse grained, they capture some spatial variability not captured by an individual remote weather station, which is commonly used (Harris and Taylor 2017; Lydersen et al. 2017). Predictor variables included Energy Release Component (ERC), Burning Index (BI), 100- and 1000-h dead fuel moistures, and wind speed (m s^{-1}). ERC is a measure of the potential heat release per unit area and corresponds to fuel moisture. BI is proportional to the expected flame length and is a product of the ERC and the predicted headfire rate of spread. BI and ERC describe important aspects of short and long-term fire weather and are related to both the expected size and intensity of the flaming front.

Topography

A 10-m DEM (Gesch et al. 2002) was processed using USDA Forest Service's FUSION v3 software package (http://forsys.cfr.washington.edu/fusion.html) to develop slope, aspect, standardized topographic position index (250-, 500-, 1000-, 2000-, and 4000-m radius windows), and solar radiation rasters.

Vegetation/live fuels

Following Parks et al. (2018b) we used several LANDSAT-derived metrics to quantify pre-fire live fuels: NDVI (normalized difference vegetation index), NDMI (normalized difference moisture index), and EVI (enhanced vegetation index). These were derived from the LANDSAT-8 imagery captured on July 14, 2013 included in the Rim Fire MTBS (Monitoring Trends in Burn Severity) data package (Eidenshink et al. 2007).

Table 3 The global list of predictor variables used in the random forest modeling of Rim Fire severity

	Resolution (m)	Source	Units
Climate normals			
Actual evapotranspiration (AET)	270	Flint et al. (2013)	mm water
Climatic water deficit (Deficit)	270	Flint et al. (2013)	mm water
Annual precipitation	270	Flint et al. (2013)	mm water
Annual temperature	270	Flint et al. (2013)	mm water
April snowpack	270	Flint et al. (2013)	mm depth
Antecedent weather[a]			
Max annual temperature (Lag 0[b], Lag 1[c])	270	Flint et al. (2013)	Degrees C
Annual precipitation (Lag 0, Lag 1)	270	Flint et al. (2013)	mm water
Annual snowpack (Lag 0, Lag 1)	270	Flint et al. (2013)	mm depth
Fire weather			
Daily energy release component	4000	Abatzoglou et al. (2013)	Unitless
Daily burning index	4000	Abatzoglou et al. (2013)	Unitless
Daily windspeed	4000	Abatzoglou et al. (2013)	m s^{-1}
Vegetation/fuels			
Normalized difference vegetation index	30	MTBS	Unitless
Normalized difference moisture index	30	MTBS	Unitless
Conifer vegetation coverage	30	LANDFIRE	Percentage
Shrub and grass coverage	30	LANDFIRE	Percentage
Non-burnable coverage	30	LANDFIRE	Percentage
Hardwood coverage	30	LANDFIRE	Percentage
Topography			
Aspect	10	USGS DEM	Cosine degree
Slope	10	USGS DEM	Percent
Solar radiation index	10	USGS DEM	Relative index
Standardize topographic position index	10	USGS DEM	Relative index
Topographic wetness index	10	USGS DEM	Unitless
Heat load index	10	USGS DEM	Unitless
Distance to road	10	TIGER	m
Fire history			
Maximum previous RdNBR	30	MTBS	Unitless
Time since last fire	30	MTBS	Years
Number of previous fires	30	MTBS	Count
Distance to past fire edge (< 10 year)[d]	30	MTBS	m
Management			
Any management, mechanical treatment, surface treatment	NA	FACTS/CAL FIRE	Yes/No
Mechancial treatment, mechanical treatment + surface treatment	180 (radius)	FACTS/CAL FIRE	Percentage
Spatial autocorrelation			
PCNM vectors 1 – 10[e]	270		Unitless

Predictor variable names in italics were included in at least one of the final models after variable selection

[a]Antecedent weather variables were represented as percentile values calculated from 1969–2013

[b]Year of the fire (2013)

[c]Year prior to the fire (2012)

[d]Only fires that occurred < 10 years prior to the Rim Fire were included

[e]Principal coordinates of neighborhood matrices (PCNM), see text. For Yosemite PCNM 6 was selected and for Stanislaus PCNM 3, 4, 5, and 8 were selected

We assessed pre-fire vegetation using the 2012 LANDFIRE existing vegetation type (EVT) layer (LANDFIRE 2012). Data were incorporated into the analysis in two forms: (1) a classification of the EVT into conifer, hardwood, shrub/grass, and non-burnable types, and (2) the percentage of each type within a 180-m radius around each pixel. We used the latter to evaluate the vegetation conditions within a local neighborhood which may influence fire effects.

Mechanical thinning and surface fuel treatments

Past harvest and fuel reduction treatment records from 1995 to 2013 were downloaded from the US Forest Service Activity Tracking System (FACTS) for the Stanislaus NF and from the California Department of Forestry and Fire Protection for Tuolumne and Mariposa Counties. Management activities were classified as clearcut, salvaged, shelterwood, and fuels reduction thinning (4 classes). Each category was also distinguished using post-harvest prescribed burning or mechanical surface fuel manipulation leading to a total of 12 classes (4 forest treatment classes $\times$ 3 surface fuel treatments (none, burn, mechanical)). These data were reclassified as any management (yes/no), mechanical treatment (yes/no), surface treatment (including broadcast burning and other mechanical treatments; yes/no), percentage area thinned (180-m window), percentage area thinned + surface treatment (180-m window).

Spatial autocorrelation

Predictor variables obtained from a principal coordinates of neighbor matrices (PCNM) were used to represent SA (Borcard and Legendre 2002; Dray et al. 2006). The PCNM procedure, a special case of spatial eigenvector maps, creates a truncated Euclidean distance matrix for points within a predefined distance, which is submitted to a principal coordinates analysis, and all eigenvectors with positive eigenvalues are returned. These vectors form fine- to broad-scale regions of spatially correlated values (Figs. S2–S4). Low-order PCNM vectors represent broad-scale SA, while higher-order vectors represent more fine-scaled SA (Borcard and Legendre 2002). These variables allowed the model to capture (1) non-stationarity in predictor-response relationships (Dormann et al. 2007), (2) unmeasured or unobservable variation in fire severity patterns, and (3) SA inherent to contagious fire spread.

Several studies have incorporated spatial eigenvector mapping into machine learning models including MAXENT (De Marco Jr et al. 2008; Blach-Overgaard et al. 2010; Reshetnikov and Ficetola 2011; Václavík et al. 2012; Cardador et al. 2014), boosted regression trees (Huang and Frimpong 2015), neural networks (Komac et al. 2016), and random forest (Ryo et al. 2018).

Truncated distance matrices were developed with a threshold distance of 10,000-m based on Moran's I correlograms of RdNBR (Fig. S1). From initial data exploration, we found that lower-ordered (e.g., 1–10) PCNM vectors consistently showed the highest variable importance. Given the computational time and system memory required to run PCNM on large matrices (Dormann et al. 2007), we calculated the first 30 PCNM eigenvectors for each of the four model runs, which captured broad- to medium-scale spatial patterns. The number of PCNM variables included in each of the four models was further reduced using feature selection ("Variable reduction and model selection").

PCNM analyses was conducted in R using scripts modified from the "pcnm" function in the vegan package (Oksanen et al. 2018). The "eigs_sym" function from the RSpectra package (Qiu and Mei 2018) replaced the base "eigen" function, which calculated only the top N eigenvectors with the largest algebraic eigenvalues. This greatly reduced computational time, and produced identical results to the base "eigen" function.

Data sampling

We further addressed potential SA in our data using gridded sampling. All data layers were sampled on a grid at various spacing intervals (30-, 60-, 90-, 180-, 270-, 360-m). From initial modeling, we decided upon 270-m spacing, which matched the resolution of the downscaled BCM climate data. Sample points within 100-m of the fire boundary were removed to reduce edge effects (Parks et al. 2018b).

Sampling points were further screened to remove the very highest (RdNBR $>$ 1200) and very lowest (RdNBR $<-$ 100) severity values to avoid outliers in the distribution, similar to Lutz et al. (2011). These represented $<$ 3% of the total number of sample

points. Sample points were also removed if they corresponded with a non-burnable substrate such as rock, water, ice, or other barren land type (LANDFIRE 2012).

Machine learning modeling

Random forest models were developed separately for the four scenarios. Modeling was conducted in the R 3.5.1 statistical software (R Core Team 2018) using the mlr package (Bischl et al. 2016). Variable importance was assessed with conditional RF models using the "cforest" function from the party package. Conditional RF uses hypothesis testing to determine variable significance at each split based on the null hypothesis of independence between predictor and response variables (Strobl et al. 2007, 2008). We found higher error rates for conditional RF models compared to the original RF implementation and therefore used (1) conditional RF for all analyses related to variable importance and (2) RF for model predictions, error-rates, and partial plots. We used default settings for RF, but increased the number of trees from 500 to 2500 to ensure stability in variable importance metrics.

Variable reduction and model selection

The goal of variable reduction was to (1) reduce the number of predictor variables (Table 3) to a parsimonious set (Table S2), (2) allow direct comparisons of predictor variables across models, and (3) retain variables within predictor variable groups representing fire-weather/climate, topography, fuels, past wildfire history (reburns only), and management (Stanislaus NF only), such that each group is represented in the final models.

We performed variable reduction separately for each of the four models resulting in four subsets of predictor variables. We then combined variable sets across models to allow for a direct comparison of predictor variable importance and their relationship to fire severity patterns. Variable reduction began by removing multicollinearity among predictor variables ($|r| \geq 0.7$). Correlated variables with higher Pearson's r coefficient with RdNBR were retained. Backwards elimination was used to identify a parsimonious set of predictor variables for each model whereby variables with the lowest importance were sequentially eliminated until final model R^2 fell below 95% of the maximum R^2. The 95% cutoff was selected to balance model performance and parsimony and corresponded with a threshold where fewer variables greatly reduced model performance. Final variables selected across all four models were combined and included in all four models with the exception of management variables, which were specific to Stanislaus NF, and past fire history variables, which were specific to reburned areas.

Due to relatively low importance when considering the entire dataset of 30-m pixels, topographic and management variables were excluded during variable reduction. However, given our model objectives, we were interested in determining if strong local importance could be identified for these variables and in quantifying the amount of shared and pure variance attributed to each variable group. Therefore, we included two topography variables, STPI (4000-m window) and slope, based on their inclusion in previous research (Kane et al. 2015b; Harris and Taylor 2017), and four management variables (Table S2).

Following variable reduction, the PCNM eigenvector 6 was selected for both Yosemite NP models, and PCNM vectors 3-5, and 8 for Stanislaus NF, which represented SA at scales between 2 and 9-km for fire-excluded areas and 7–12-km for reburns (Fig. S4). Variable reduction procedures are commonly applied in regression analyses to eliminate nonsignificant PCNM vectors (Borcard and Legendre 2002; Bellier et al. 2007; Hernández-Stefanoni et al. 2011). In lieu of statistical significance measures for the RF models, we determined that the limited number of PCNM predictors selected by variable reduction sufficiently removed extraneous SA variables.

Local variable importance

Predictor variable importance was further assessed at individual sample points using the mlr package (Bischl et al. 2016). Local importance values were scaled such that all values < 0 (low importance) were converted to NA and remaining values were scaled between 0 (lowest)–100 (highest) using a linear transformation. Scaled values were subsequently mapped for further inspection.

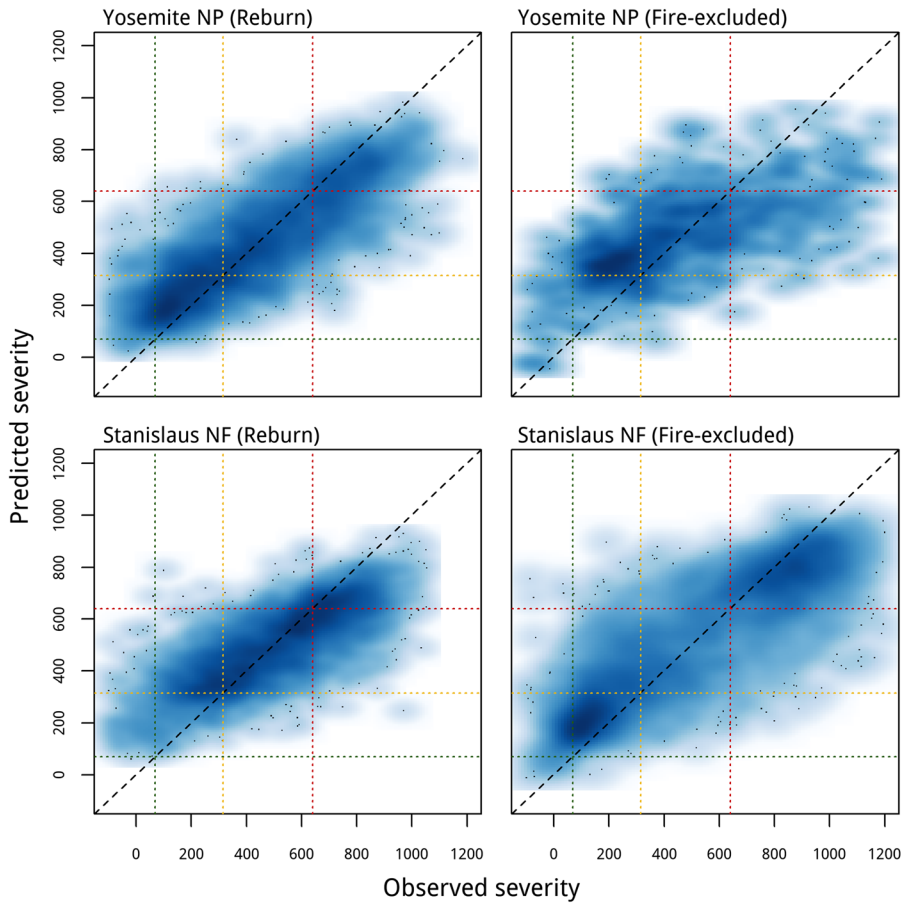

Fig. 3 Observed Rim Fire severity (RdNBR) versus out-of-bag random forest model predictions. Blue shading represents a 2-dimensional kernel density estimate with darker hues representing higher densities of observations. Black diagnol dashed line repesents the 1:1 line where predictions are equivalent to the observed severity. Dotted lines represent fire severity class cutoffs: low (green), moderate (yellow), and high (red). (Color figure online)

Variance partitioning

Variance partitioning develops factorial combinations of predictor variables or variable groups, and calculates the pure, shared, and total variance explained among them (Borcard et al. 1992). Pure variance refers to the individual contribution of a variable group, while shared variance is jointly accounted for by more than one group. Predictor groups included climate/weather, topography, fuels (i.e., fire history, NDVI and NDMI), and spatial autocorrelation (Table S2). These methods were conducted using out-of-bag model R^2 for RF models with scripts modified from the varpart function within the vegan package (Oksanen et al. 2018).

Variance partitioning is generally used with linear models, rather than machine learning algorithms (Chen 2015). The important distinction is that most machine learning algorithms incorporate interactions among variables while linear models are additive. Recently, variance partitioning methods have been extended to include regression trees (Boone and Krohn 2000; Bucini et al. 2009), and boosted regression trees (Quisthoudt et al. 2013; Feld et al. 2016; Lemm et al. 2019). To test the effect of RF on variance partitioning results, we re-ran variance partitioning with generalized additive models (GAM). GAMs are flexible and capable of modeling non-linear relationships, but combinations of predictors are additive rather than interactive as is the case for RF.

Table 4 Sample sizes (i.e., number of pixels used as training data) and out-of-bag R^2 for random forest models used to model Rim Fire severity

Ownership	Fire-type	Sample size	R^2_{OOB}
Yosemite NP	Reburned	3703	64.5
Yosemite NP	Fire-excluded	716	41.4
Stanislaus NF	Reburned	4234	56.7
Stanislaus NF	Fire-excluded	2988	64.5

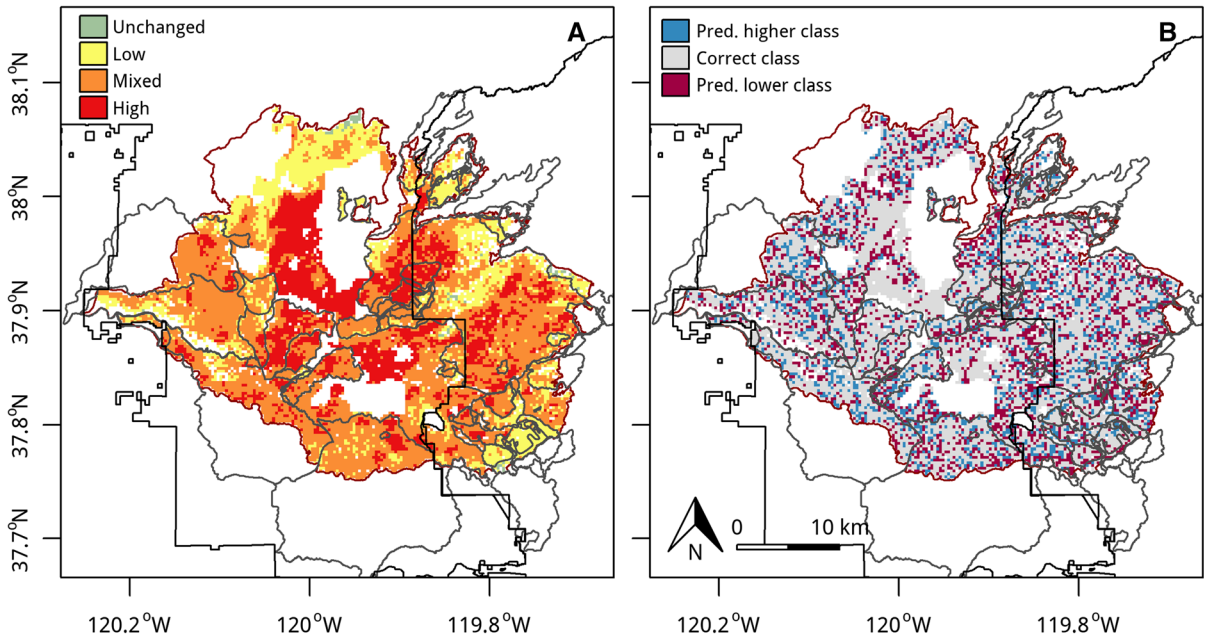

Fig. 4 **a** Random forest predicted Rim Fire severity (RdNBR, 270-m resolution), reclassified into fire severity class bins, and **b** classified model residuals. Areas within the Rim Fire without predictions are where fire burned previously before 1984 and no RdNBR data existed for these fires. Grey solid lines represent boundaries of previous fires that burned between 1984–2012. Black lines depict the boundaries of the Stanislaus National Forest to the west and Yosemite National Park to the east

Results

Model performance

For Yosemite NP, the reburn model had a higher out-of-bag R^2 (64.5%) compared to the fire-excluded model (41.4%; Fig. 3; Table 4). However, for Stanislaus NF the model for fire-excluded areas had a higher out-of-bag R^2 (64.5%) compared to the reburn model (56.7%). Models generally over-predicted the unchanged and low severity classes and under-predicted the high severity class (Fig. 3). Spatial trends in model predictions showed that models were accurate for general trends in fire severity patterns, but were not sensitive to much of the fine-scaled patterning associated with non-plume dominated days (Fig. 4). Differences between the observed (30-m) and predicted (270-m) severity maps (Figs. 2, 4) can partially be attributed to the coarser resolution of the training data. Moran's I correlogram showed moderate levels of SA in Rim Fire RdNBR, which was effectively removed in the RF residuals both with and without the SA variables (Fig. S1).

Predictor variable importance

Key differences were apparent in model variable importance across Stanislaus NF and Yosemite NP

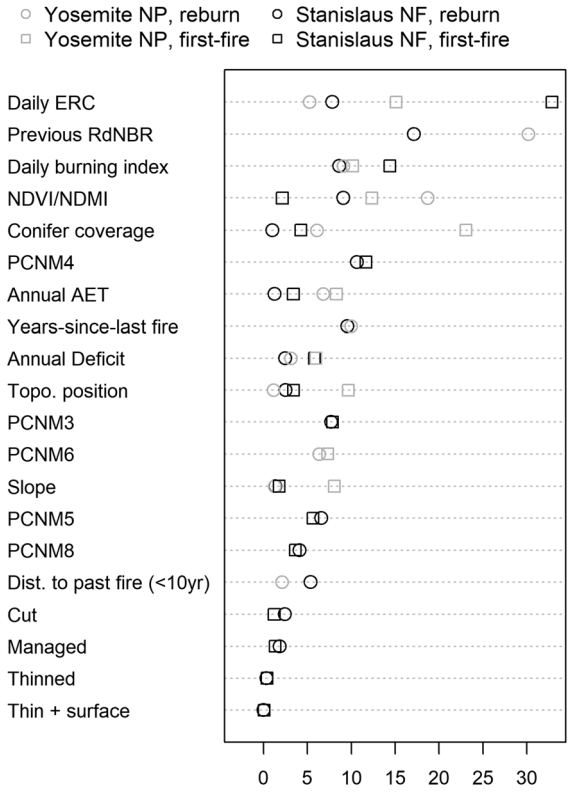

Fig. 5 Dotplot depicting the relative variable importance for the four random forest models used to model Rim Fire severity. Abbreviations are: *RdNBR* relativized differenced normalized burn ratio, *ERC* energy release component, *NDVI* normalized difference vegetation index, *NDMI* normalized difference moisture index, *PCNM* principal coordinates of neighborhood matrices, *AET* actual evapotranspiration

(Figs. 5, 6, 7). For fire-excluded areas, fuels variables (conifer cover and NDVI) were the most important drivers of severity in Yosemite NP, while daily fire weather and SA variables were most important in Stanisluas NF (Figs. 5, 6). For both models, daily fire weather variables were of greater importance than long-term climate variables, and topography variables had low importance overall (Figs. 5, 6).

For reburned areas, previous fire severity was the main driver for both Yosemite NP and Stanislaus NF, and severity increased linearly with previous RdNBR. However, variable importance for previous RdNBR was much higher for Yosemite NP (Figs. 5, 7). Similar to fire-excluded areas, fuels variables tended to have higher variable importance in Yosemite NP, and SA variables were more influential in Stanislaus NF. Topography variables were similarly poor predictors overall. Daily fire weather variables were comparatively less important for reburn models (Figs. 5, 7). Forest management variables showed low overall variable importance regardless of the management action for both reburned and fire-excluded areas (Fig. 5).

Spatial autocorrelation variables generally had higher importance for Stanislaus NF models compared to Yosemite NP (Figs. 5, S4–S6). Response curves for SA variables were generally non-linear, but note that there are no a priori functional relationships between these variables and RdNBR as the PCNM axes represent purely spatial trends (Figs. S5, S6).

Local drivers of fire severity

For fire-excluded areas, fire weather was the dominant variable in Stanislaus NF for both plume and non-plume dominated days, with some areas of high fuels importance near the Clavey and Tuolumne Rivers (Figs. 8, S1). In Yosemite NP, fuel was the most important variable for fire-excluded areas followed by fire weather, which were located at the southeastern border of the fire outside of the plume-dominated burn days (Fig. 2b, c).

For reburned pixels, previous fire history was the main driver of fire severity for Stanislaus NF and Yosemite NP under both plume and non-plume dominated days (Fig. 8). However, fire history variables had weak importance in a large area near the boundaries of the Stanislaus NF and Yosemite NP near the center of the fire. This area corresponded with high importance for weather variables in the Stanislaus NF, with mixing of high importance for fuels (NDVI, conifer coverage) and weather variables in Yosemite NP.

Overall, topographic variable importance was low, but increased near rivers and lakes, and for isolated patches dispersed throughout the fire extent. For instance, near the center of the Stanislaus NF, high topographic variable importance corresponded with a large depression (low STPI) among rolling terrain dissected by a riparian area (Fig. 8), which experienced comparably lower fire severity than surrounding areas (Fig. 2).

Evidence of effective past management was apparent for some isolated treatment units near the Yosemite NP boundary, near the Clavey River, and between Cherry and Eleanor Lakes (Figs. 8, S1). Near

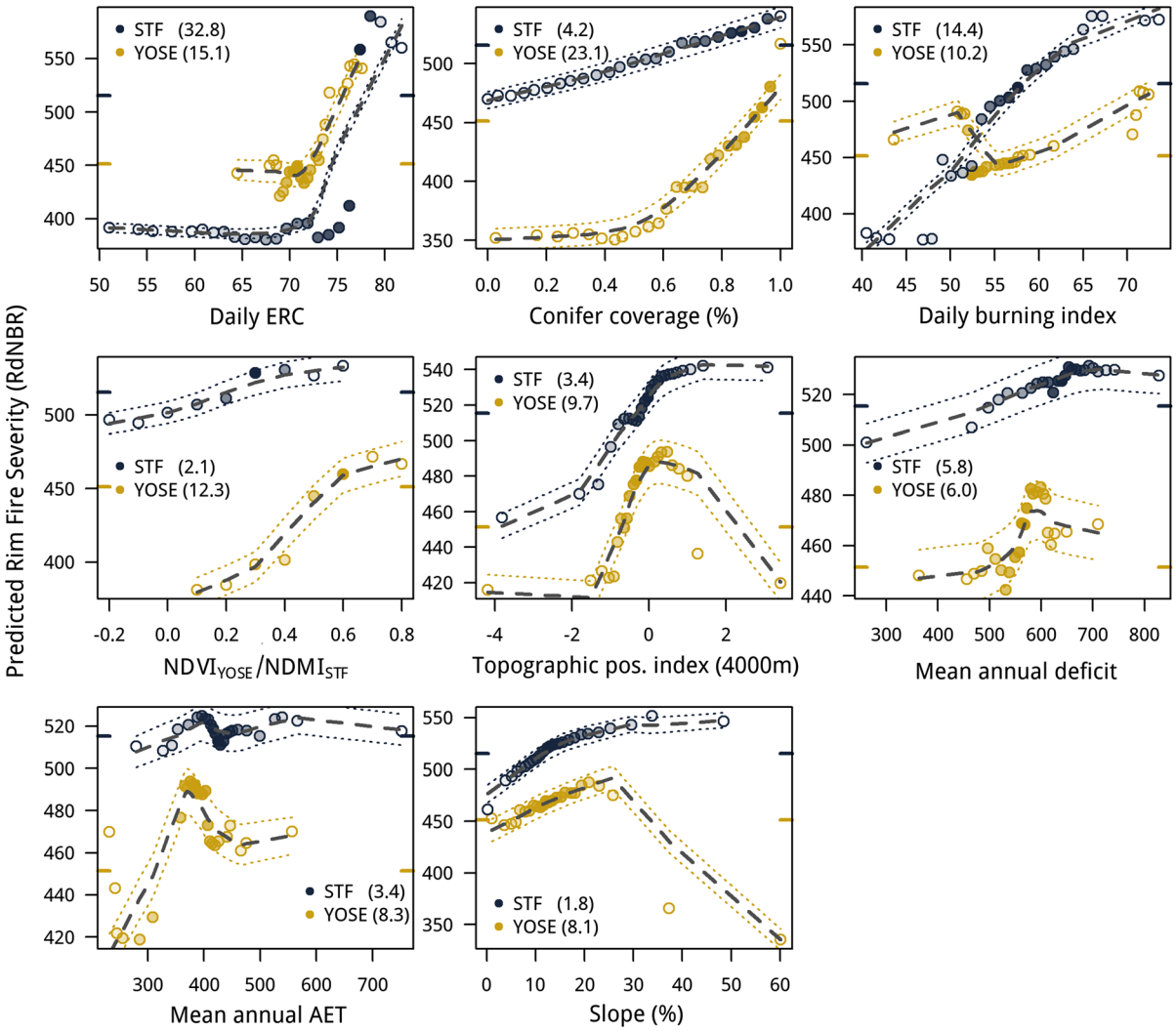

Fig. 6 Partial dependence plots for the top 8 predictor variables (excluding SA variables) for random forest models used to evaluate fire-excluded areas (e.g., areas that burned during the 2013 Rim Fire for the first time on record). Plots depict the marginal effect of a predictor variable on predicted Rim Fire severity. Points represent severity predictions made for 25 values across the range of each predictor variable. Dashed grey lines are lowess (locally weighted scatterplot smoothing) smoothed trend lines, and colored dotted lines are 2 * SE of the lowess estimate. The opacity of each point was determined by the empirical density function of the predictor variable with darker hues representing higher densities and lighter hues representing sparse data. Values in parentheses represent variable importance for Stanislaus NF (STF) and Yosemite NP (YOSE), and panels are ordered by the mean variable importance. Blue and gold tick marks on plot margins indicate the mean fire severity for STF (blue) and YOSE (gold). (Color figure online)

the southeastern border of Stanislaus NF, a large treated area, consisting of a > 700-ha commercial thin ~ 16–18 years prior to the fire and a > 400-ha clearcut following the 1996 Ackerson Fire exhibited high variable importance (Fig. 8). Both units were outside the area covered by the two most extreme plume-dominated burn days, but were affected by later plume-dominated fire progressions, which burned less severely. Near the Clavey River, a 1997 clearcut area (~ 600-ha) near the eastern extent of the 1996 Rogge Fire corresponded with high importance for management variables.

Variable importance values for management variables were lower under plume-dominated conditions

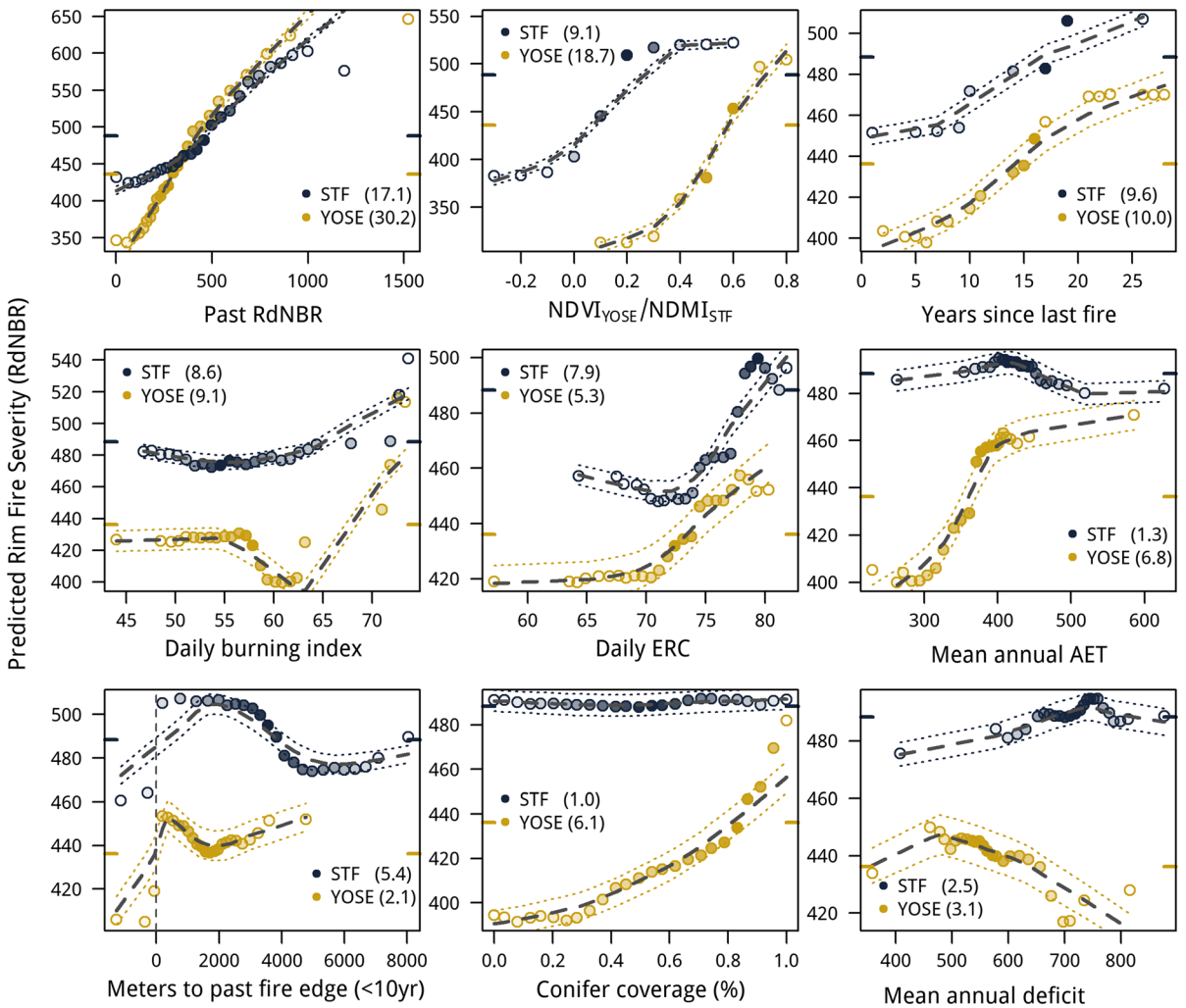

Fig. 7 Partial dependence plots for the top 9 predictor variables (excluding SA variables) for random forest models used to evaluate reburn fires (e.g., areas that burned between 1984–2012) within the 2013 Rim Fire. Plots depict the marginal effect of a predictor variable on predicted Rim Fire severity. Points represent severity predictions made for 25 values across the range of each predictor variable. Dashed grey lines are lowess (locally weighted scatterplot smoothing) smoothed trend lines, and colored dashed lines are 2 * SE of the lowess estimate. The opacity of each point was determined by the empirical density function of the predictor variable with darker hues representing higher densities and lighter hues representing sparse data. Values in parentheses represent variable importance for Stanislaus NF (STF) and Yosemite NP (YOSE), and panels are ordered by the mean variable importance. Blue and gold tick marks on plot margins indicate the mean fire severity for STF (blue) and YOSE (gold). (Color figure online)

(Fig. S7). However, where management was effective under the plume, treatments led to relatively lower fire severity compared to treatments outside the plume (Fig. S7). Spatial autocorrelation variables exhibited high importance in the southwestern portion of the Rim Fire in a reburned landscape near the Tuolumne River (Fig. 8). This area was influenced by plume-dominated fire spread and all other variable groups had low explanatory power in this region.

Variance partitioning

Variance partitioning of the RF models revealed a high level of shared variance among predictor groups, particularly with SA (Fig. 9). Much of the observed

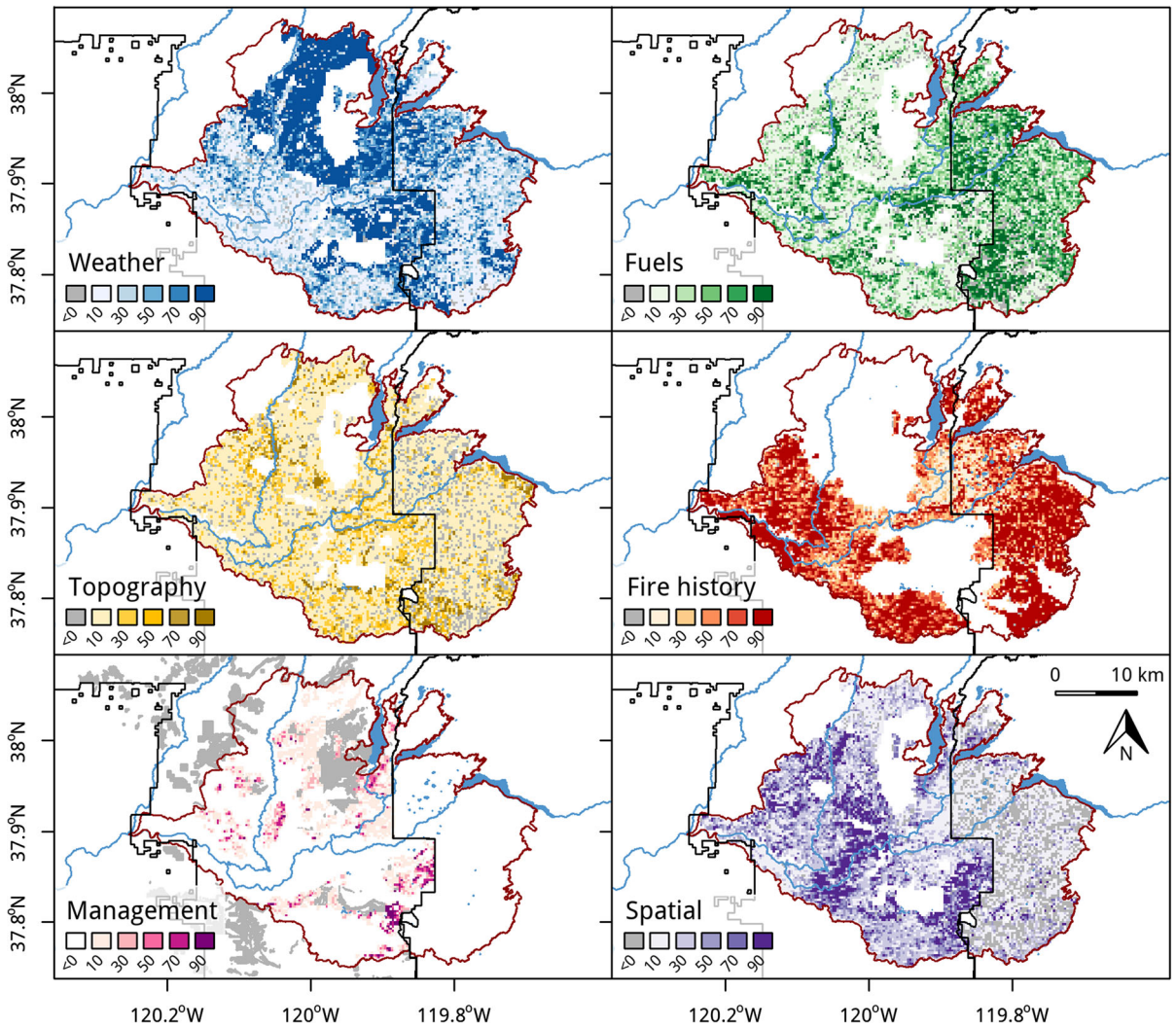

Fig. 8 Local predictor variable importance for the random forest model was used to evaluate drivers of fire severity for first-entry fires and reburns within the 2013 Rim Fire boundary (dark red line). Each raster pixel (270-m resolution) represents the relative strength of each predictor variable category with darker colors representing higher importance. Classes represent scaled local variable importance values < 0, 0–20, 20–40, 40–60, 60–80, and 80–100. Solid grey polygons in the lower left panel were managed between 1995–2012. Previous fire boundaries (1984–2012) are outlined in dark grey. Stanislaus National Forest (west) and Yosemite National Park boundaries (east) are demarcated in black lines. Lakes and major rivers are included for reference. Areas with no local variable importance metrics (i.e., white space within Rim Fire boundary) were burned prior to 1984, had no fire severity data for the previous fire and were subsequently removed from analyses. Additional white space in the "fire history" panel further removes first-entry fire area and shows only the area reburned by the Rim Fire. (Color figure online)

shared variance was between weather, fuels and SA. The level of pure variance explained by any one variable group was relatively low, and only 4–16% of the explained variance was attributable to the pure variance explained by climate/weather, topography, and fuels variable groups. Pure variance explained was generally higher in reburn models compared to models for fire-excluded areas.

Compared to the RF modeling, GAM models exhibited lower overall variance explained, but much of this difference was due to a reduction in shared variance between SA, fuels, and weather in the GAM models (Fig. S9). For example, for fire-excluded areas

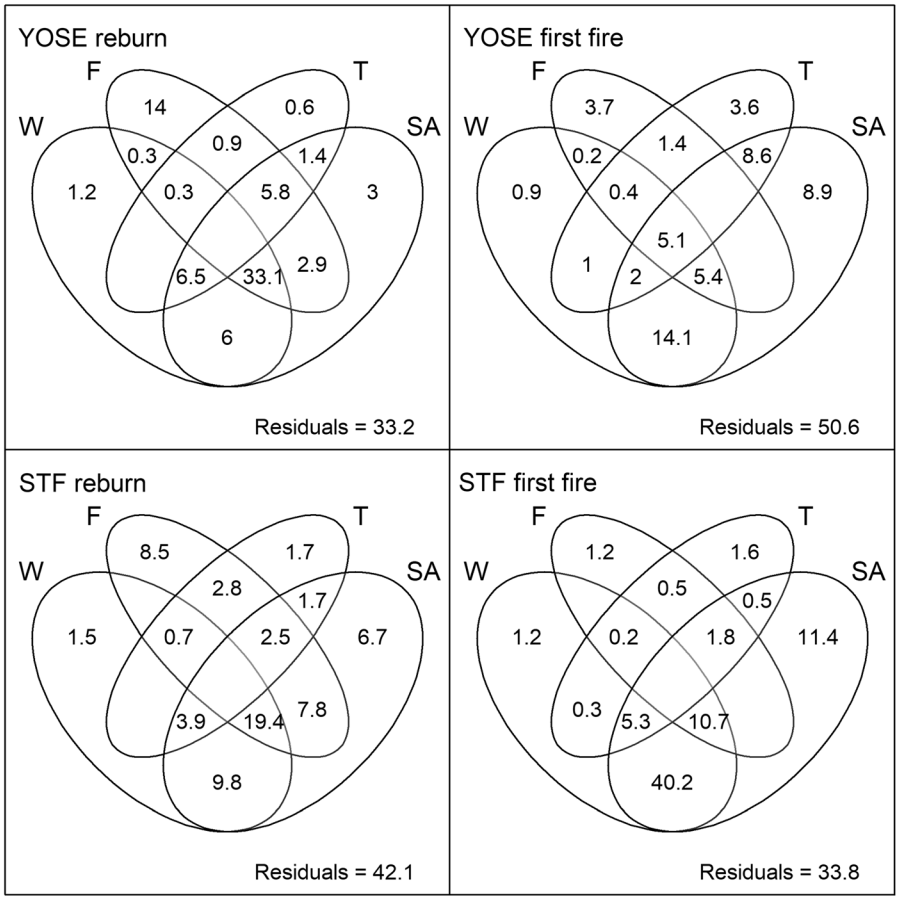

Fig. 9 Variance decomposition plot depicting the percentage of the out-of-bag variance explained by random forest models for individual predictor variable groups (non-overlapping regions) and shared among predictor variable groups (overlapping regions). Residuals are the remaining variance left unexplained by each model and is equal to $100 - R^2$. Variable groups are: *W* weather, *F* fuels, *T* topography, *SA* spatial autocorrelation. See Table S2 for a list of the variables included in each group

in Stanislaus NF, shared variance among weather, fuels, and SA totaled 56.2% for RF models, but only 34% for GAM models. Similarly, shared variance for RF models in reburned areas of Stanislaus NF was 33.1% compared to only 8.1% for GAM models. Similar trends were found for Yosemite NP reburns (45.6% RF; 21.8% GAM) and fire-excluded areas (21.5% RF, 15.3% GAM).

Discussion

Our results demonstrate that wildfires are inherently a multi-scaled process driven by top-down and bottom-up factors, similar to findings across the western US (e.g., Estes et al. 2017; Parks et al. 2018b). The results revealed a diverse mixture of environmental controls on fire severity that varied markedly across burn periods, environmental gradients, and land ownerships. Reliance on global variable importance measures and response curves that display average trends limits understanding of the local controls that mediate fire severity and contribute to landscape heterogeneity. Modeling methods should capture both the complex relationships between drivers of fire severity patterns and the spatial non-stationarity in the magnitude and direction of these relationships.

Top-down controls on Rim Fire severity patterns

Fire weather was a dominant driver of severity in Stanislaus NF, particularly where the Rim Fire burned in areas where fire was excluded for > 80 years. These areas generally burned under the two largest plume-dominated burn days where 47% of pixels burned with high severity compared to 21% for all other burn days. Bottom-up factors played a minimal role in mitigating fire severity during this time, but provided some local control throughout. However, simply interpreting the pattern of observed fire effects during plume-dominated fire spread as evidence of top-down control is not entirely appropriate. Plume formation is the result of teleconnections between combustion at the surface and atmospheric conditions (Werth et al. 2016). The effect of fire exclusion on fuel loads and continuity over much of the Stanislaus NF likely contributed to accelerated heat release rates, which may have influenced observed plume dynamics (Peterson et al. 2015, 2018). In this light, the "plume effect" represents an interesting interaction between top-down and bottom-up controls, which merits further research.

Other top-down climatic variables including long-term AET and water deficit (30-year normals) were weakly related to severity, which was also reported by Harris and Taylor (2017) for reburns within the Rim Fire extent. The Rim Fire occurred during the historic 2012–2015 drought, which corresponded with severely reduced precipitation, snowpack, streamflow and soil moisture levels (Funk et al. 2014; Griffin and Anchukaitis 2014). These conditions likely led to low moisture content in live and dead surface and canopy fuels with relatively low spatial variability across the landscape (Asner et al. 2016), weakening the influence of climatic variation on fire effects.

Bottom-up controls on Rim Fire severity

Previous fire history

Bottom-up controls provided by previous burns were dominant across reburned areas, similar to other Rim Fire studies (Kane et al. 2015a; Harris and Taylor 2017; Lydersen et al. 2017) and elsewhere in the Sierra Nevada (van Wagtendonk 2012; Coppoletta et al. 2016). We found a strong linear relationship between past severity and Rim Fire severity, indicating that fire severity is self-reinforcing (van Wagtendonk et al. 2012; Kane et al. 2015a; Harris and Taylor 2017; Lydersen et al. 2017). Importantly, we found that these patterns held for reburns under both plume and non-plume dominated burn periods, emphasizing the strength of previous fire as a bottom-up control in these ecosystems even under extreme fire weather conditions.

Our results suggest that high-severity fire is self-reinforcing in these landscapes and can occur independent of strong top-down factors such as severe weather conditions, particularly where time-since-last fire exceeded 10–15 years. Parks et al. (2014) suggest possible pathways for self-reinforced high-severity fire. Firstly, repeated high severity fires in shrubland types, which represented ~ 8% of the Rim Fire burned area, are generally self-replacing under a high-severity regime. Secondly, post-fire conversions from forest to shrubland can perpetuate where fires return prior to forest re-establishment (van Wagtendonk et al. 2012; Lydersen et al. 2014; Coppoletta et al. 2016). For example, Lydersen et al. (2014) showed that, under mild fire weather, the Rim Fire burned at higher severity where shrub cover exceed 22%. Thirdly, heavy fuel loads and/or dense post-fire regeneration within high severity patches can cause subsequent high severity fire. In the northern Sierras, Coppoletta et al. (2016) found that high- and moderate-severity fire patches led to increases in both shrub and standing snags, which contributed to subsequent high-severity fire. While the contribution of these fuels is unclear from remotely sensed vegetation, Lydersen et al. (2014) showed that Rim Fire severity increased with increasing time-since-fire, particularly where past burns occurred > 14 years prior, suggesting that post-fire vegetation and fuel dynamics over time likely contributed to increased risk of high severity fire. Our findings, along with those of Kane et al. (2015a) and Harris and Taylor (2017), also showed severity increased with time-since-last fire, with more pronounced increases in fire severity after 10–15 years, corroborating the results of Lydersen et al. (2014) across the whole of the Rim Fire area.

Fuels

Fuels variables exhibited higher overall importance in Yosemite NP compared to Stanislaus NF. In Yosemite NP, our fuel proxies (conifer cover and NDVI) were

the main drivers throughout much of the fire extent, even within some portions of the plume-dominated spread. Spatial maps of predictor variable importance showed that within a single burn period, fire effects shifted from weather-dominated in Stanislaus NF in favor of fuels and fire history variables in Yosemite NP, possibly as a result of reduced surface and canopy fuels in the park resulting from recent prescribed and managed fires. These fuel changes may have precluded strong plume formation, though more research is needed to explore these dynamics. Forest structure differed between ownerships, particularly in the greater abundance of large trees in the NP (Collins et al. 2017a), which are more resistant to fire-related mortality due to increases in canopy base heights and thicker bark (Lentile et al. 2006). In addition, management of Yosemite NP incorporated a considerable amount of fire use, through both prescribed fire and allowing natural fire starts to burn under less-than-extreme weather conditions (Miller et al. 2012). Together, these factors have promoted forest structure that is more similar to that observed under an active-fire regime (Lydersen and North 2012), despite aggressive fire suppression prior to the mid-1970s (van Wagtendonk 2007).

Topography

Topography provided weak bottom-up controls on fire severity overall, but evidence of local importance for topographic variables was exhibited throughout the Rim Fire. This contrasts with past research that suggests a strong role for topographic variables in explaining fire severity (Alexander et al. 2006; Holden et al. 2009; Harris and Taylor 2015, 2017; Estes et al. 2017) and fire spread (Coen et al. 2018; Povak et al. 2018) patterns. The role of topography is complex as it provides both direct (i.e., convective heating on steep slopes) and indirect (e.g., changes in solar regimes, vegetation, and soils) influence on fire behavior (Heyerdahl et al. 2001; Alexander et al. 2006; Holden et al. 2009; Estes et al. 2017). The weak role of topography in our study suggests that indirect controls on vegetation, fuels and microclimate conditions were better captured by those spatial variables directly (Lydersen and North 2012; Kane et al. 2015b; Coppoletta et al. 2016; Estes et al. 2017; Parks et al. 2018b). Variance partitioning in our study showed that fuels and weather variables exhibited a similar amount of shared variance with topographic variables, suggesting that topography influenced patterns of both variables equally with respect to their control on fire severity patterns. High local importance for topographic variables in our study generally corresponded with lower fire severities and occurred along topographic breaks (e.g., changes in aspect) that presented barriers to fire spread (Meddens et al. 2018; Blomdahl et al. 2019), as well as topographic depressions and riparian areas that likely mitigated fire severity through increases in soil moisture and localized cold-air pooling (Lundquist et al. 2008; Minder et al. 2010; Van de Water and North 2010). Results demonstrate how local importance maps can identify topographically enforced fire refugia that can provide important post-fire seed sources and habitat (Camp et al. 1997; Meddens et al. 2018; Martinez et al. 2019).

Mechanical treatment effects

Mechanical treatments showed low global importance in RF models, but local effectiveness of mechanical treatments was observed in portions of the NF. The limited area affected by management ($\sim 8\%$ of Stanislaus NF within the Rim Fire extent) and even lower incidence of fuels reduction treatments may have precluded finding important effects of specific treatments on fire severity. In addition, NDVI and NDMI variables may implicitly incorporate the effect of management activities, which may better capture the vegetation response to management and remove the effect of categorical treatment variables (Parks et al. 2018b). The variable importance for mechanical treatments was higher outside of plume-dominated progression intervals suggesting that treatment effectiveness is likely greater under milder burning conditions. However, where treatment variables had high local importance, treatments within the plume were shown to have a greater relative effect at reducing fire severity compared to treated areas outside the plume-dominated spread, particularly for fire-excluded areas (Fig. S7). Similarly, Prichard and Kennedy (2014) found evidence for treatment effectiveness under extreme fire weather conditions during the 2006 Tripod Complex fires in central Washington. This suggests that treatments can help mitigate fire severity even under the most extreme weather conditions, although the likelihood of effectiveness is reduced.

Relative role of weather, fuels, and topography

Despite much research into identifying drivers of fire severity, questions remain as to the relative roles of weather, fuels, and topography in driving landscape-level fire severity patterns (Parks et al. 2011; Birch et al. 2015; Fang et al. 2015; Parks et al. 2018b). Parks et al. (2018a) showed that live fuels (i.e., NDMI, and enhanced vegetation index (EVI)) were $\sim$ 2.4 times more influential than climate variation (i.e., year-of-fire climate) for predicting low-severity fire across $>$ 400 fires in the southwestern US. Similarly, Parks et al. (2018b) modeled the drivers of high-severity fire for $>$ 2000 fires across the western US and found that live fuels were $\sim$ 2.3 times more influential than fire weather variables, though substantial ecoregional variation existed.

Results from our variance partitioning analyses were more equivocal due to the high levels of shared variance exhibited across variable groups. Much of the variance explained was shared between SA, weather, and fuels variable groups. Parks et al. (2011) similarly showed that statistical models of simulated burn probability exhibited high shared variance among elevation, ignitions and fuels predictors. The authors concluded that high shared variance complicates model interpretation and can potentially lead to counterintuitive relationships. Statistical modeling methods should therefore be employed to tease apart the relative strength of these feedbacks, which may help reveal contributions of top-down and bottom-up drivers to fire severity patterns.

Fuels variables exhibited the highest level of pure and total variance explained for reburn models, further demonstrating that landscape vegetation patterns contribute strong controls on fire behavior during large fire events (Bradstock et al. 2010; Prichard and Kennedy 2014). However, high shared variance among fuels and weather variables indicated the role of fuels in controlling fire severity is contingent upon weather conditions as has been shown previously (Collins et al. 2009; Prichard and Kennedy 2014; Stevens-Rumann et al. 2016; Prichard et al. 2017). Fuels were comparatively stronger for Yosemite NP reburns, suggesting a higher level of bottom-up controls provided by vegetation in the park, which has a higher degree of restored natural fire and legacy large trees (Johnson et al. 2013; Collins et al. 2017a). Furthermore, the relative dominance of fuels and weather variables was reversed for fire-excluded areas where fuels exhibited a much lower level of control in both land designations, possibly due to similarities in vegetation conditions across ownerships due to fire exclusion.

To our knowledge, this was the first application of variance partitioning to fire severity research, and it appears to be a promising avenue of research to disentangle relationships among drivers of severity patterns. Parks et al. (2018a, b) calculated the relative influence of variable groups as the difference in cross-validated error-rates between the full model and model subsets where variables groups were iteratively excluded. This method is an effective way to rank the relative importance of variable groups, but cannot represent shared variance among them. However, caution should be used when interpreting these results as the shared variance components may have been overexpressed by the RF models. Compared to RF, GAMs (flexible function, but with no interaction terms) showed lower total variance explained, particularly for the Stanislaus NF models (Fig. S8). Much of the loss in variance explained in the GAMs was related to the lower shared variance component (i.e., 20–36% for GAMs vs. 32–52% for RF models), while the pure variance components were similar across models. Inflated estimates of shared variance have previously been reported for boosted regression trees (similar to RF) in variance partitioning applications used to model aquatic organism populations (Lemm et al. 2019) and their stressors (Feld et al. 2016). However, Quisthoudt et al. (2013) found only slight increases in shared variance in boosted regression trees compared to linear models and GAMs. The increased accuracy provided by machine learning algorithms appear to come at the expense of model interpretability given that much of the additional variance explained is partitioned into shared variance components. However, the level of shared variance identified by the GAM models was still large, which reinforces the finding of a lack of independence among predictors. More research is needed to identify these interactions, their functional form, and their generalizability to other environments.

Spatial autocorrelation

Inferences from the spatial analyses were that (1) SA in model residuals was negligible at all scales with and

without spatial PCNM variables included in the models, (2) SA variables represented broad-scale spatial patterns ($\sim$ 10 km), and (3) long-range interdependencies among fire severity and main predictors revealed strong shared variance among SA and environmental predictors (Fig. 9). Few differences were found in variable importance, response curves, or inferences made from RF models with and without SA predictors, and SA variables only slightly increased model performance ($\leq$ 10% increase in R^2_{OOB}). Environmental predictors appeared to adequately capture SA, which runs counter to past studies that showed increased model performance and lower residual SA with spatial covariates (Crase et al. 2012). For example, Portier et al. (2018) showed that RAC models outperformed aspatial models and provided more realistic estimates of pure and shared variance among predictors. This latter point was confirmed in our analyses given that SA variables accounted for much of the shared variance among predictor groups, suggesting that estimates of the remaining shared and pure components were likely more reliable.

High levels of shared variance among environmental and SA variables also suggests that the spatial patterns of fire severity were largely influenced by the strong spatial structure of the predictor variables. This suggests that (1) environmental variables are highly interactive, (2) that gradients exist whereby gradual changes in variables create similar conditions across space, (3) fire severity is a highly non-stationary process where the relative influence of key drivers change across burn days and environments and these relationships are dependent upon their spatial context. Methods, such as SAR, that incorporate local neighborhood SA into the model (Prichard and Kennedy 2014) may miss important broad-scale spatial dependencies, which require a multi-scaled assessment of SA to capture. We speculate that broad-scale patterns were predominantly driven by changes in weather conditions across burn periods that led to severe or benign fire behavior (Hammill and Bradstock 2009; Bradstock et al. 2010; Coen et al. 2018), particularly in the fire-excluded areas. Plume-dominated fire behavior in these areas led to large patches of high severity fire, creating a broad-scale pattern of similar severity, consistent with patterns observed for recent fires across California (Stevens et al. 2017; Steel et al. 2018). Across the remaining burn periods, severity was lower overall, patch sizes were smaller, and exhibited a greater intermixing of fire severities. These patterns are also characteristic of fire-use wildfires that burn under moderate conditions for their ecological benefits and are similar to historical patterns (Mallek et al. 2013; Meyer 2015).

Conclusions

We assessed spatial patterns of fire severity for the 2013 Rim Fire and quantified the relative role of weather, topography, fuels, and spatial autocorrelation on explaining fire severity patterns within fire-excluded and reburned areas. Our methods extended those of previous studies (Kane et al. 2015a; Harris and Taylor 2017; Lydersen et al. 2017) to (1) quantify the relative role of top-down and bottom-up controls, (2) map spatial patterns of predictor variable importance, (3) compare drivers across managed (Stanislaus NF) and unmanaged (Yosemite NP) lands, and (4) assess the relative role and scale at which spatial autocorrelation influences model results.

Our results show that while fire weather was an important driver of high severity fire, weather variables were most influential in fire-excluded areas. One explanation for this is that fuels are more uniformly high in long fire-excluded areas, and as a result did not vary enough to warrant strong statistical influence. While fire suppression activities have influenced both Yosemite NP and Stanislaus NF, the latter had appreciably more area untouched by recent fire. Within the Rim Fire footprint, approximately 22,800 ha (32%) were fire excluded (> 80 years) in Stanislaus NF compared to 6000 ha (19%) in Yosemite NP. These fire-excluded areas often corresponded with—and possibly contributed to—extreme plume-dominated fire severity (Peterson et al. 2015; Werth et al. 2016), which usurped most bottom-up controls and created large high-severity patches. However, evidence of local bottom-up controls was identified throughout the fire extent suggesting that strong top-down control from fire weather can be overridden by local patterns of topography, vegetation, and fuels (Safford et al. 2012; Prichard and Kennedy 2014). Reburned areas showed strong bottom-up controls from previous burns suggesting a high degree of landscape memory and feedbacks in the system whereby reburn severities were similar to the

previous fire (Collins et al. 2009; Parks et al. 2014; Harris and Taylor 2017; Lydersen et al. 2017). Fuels also played a dominant role in Yosemite NP, where lower overall fire severity was associated with a history of prescribed and fire-use fires along with the presence of large, old trees, which likely contributed to high resiliency (Thompson and Spies 2009; Collins et al. 2017a). Accordingly, local variable importance results presented here corroborated recent anecdotal evidence that plume-dominated fire spread weakened once the fire reached portions of Yosemite NP that had experienced past fires (Keeley and Syphard 2019). The variability in both fire severity and predictor variable importance emphasizes a need to more explicitly characterize spatial patterns within individual wildfires (e.g., Collins et al. 2017b) rather than labeling them as "extreme events" or "megafires". These labels connote homogenous, and often negative, impacts, which is not always the case (Rollins et al. 2002; Hammill and Bradstock 2009; Keane et al. 2009; Bradstock et al. 2010; Lydersen et al. 2014; Harris and Taylor 2017). Furthermore, strong shared variance across predictor variable groups suggests a high-level of cross-talk among bottom-up and top-down factors and signals important teleconnections within and among terrestrial and atmospheric processes that may be indicative of large fires.

Results confirm that low- and moderate-severity fire can mitigate subsequent wildfire severity, even under extreme fire weather, regardless of past management history. In these environments, prescribed burning alone, or as a surface treatment following mechanical operations, has high utility in restoring historical fire regime properties and concomitant ecological processes, as well as allowing forests to adapt to future predicted increases in temperature and drought (Williams et al. 2015).

Models that rely on global variable importance and response curves that display average trends can obfuscate the importance of local controls. Maps of predictor variable importance revealed tradeoffs between bottom-up and top-down factors. For example, topography and recent management variables showed high importance in some localized areas despite exhibiting low variable importance overall (Fig. 5). Such information can improve our understanding of the conditions under which bottom-up controls provide buffers or barriers to fire severity and spread, help prioritize landscape treatments, and inform fire suppression efforts.

Spatial autocorrelation analyses revealed broad-scale spatial dependencies in pattern-process linkages up to $\sim$ 10-km. High levels of shared variance among weather, fuels, and spatial autocorrelation variables suggested that drivers of fire severity are highly interactive, and exhibit strong, broad-scale spatial structure. Fine-scaled heterogeneity within these larger patterns occurred where unique combinations of bottom-up factors collectively mediated severity. Such information is invaluable for directing spatial locations and arrangements of future restoration treatments, which should be the focus of future research.

Acknowledgements This research was funded through grant #14-1-01-23 of the Joint Fire Sciences program. This project was supported in part by an appointment to the Internship/Research Participation Program at the Pacific Northwest Research Station, U.S. Forest Service, administered by the Oak Ridge Institute for Science and Education (ORISE) through an interagency agreement between the U.S. Department of Energy and U.S. Forest Service. The authors thank Susan Prichard and Brion Salter for their thoughtful and thorough reviews of the manuscript.

References

Abatzoglou JT (2013) Development of gridded surface meteorological data for ecological applications and modelling. Int J Climatol 33:121–131

Alexander JD, Seavy NE, Ralph CJ, Hogoboom B (2006) Vegetation and topographical correlates of fire severity from two fires in the Klamath-Siskiyou region of Oregon and California. Int J Wildland Fire 15:237–245

Asner GP, Brodrick PG, Anderson CB, Vaughn N, Knapp DE, Martin RE (2016) Progressive forest canopy water loss during the 2012–2015 California drought. Proc Natl Acad Sci USA 113:E249–E255

Barbero R, Abatzoglou J, Larkin N, Kolden CA, Stocks B (2015) Climate change presents increased potential for very large fires in the contiguous United States. Int J Wildland Fire 24:892–899

Beaty RM, Taylor AH (2001) Spatial and temporal variation of fire regimes in a mixed conifer forest landscape, Southern Cascades, California, USA. J Biogeogr 28:955–966

Bellier E, Monestiez P, Durbec J-P, Candau J-N (2007) Identifying spatial relationships at multiple scales: principal coordinates of neighbour matrices (PCNM) and geostatistical approaches. Ecography 30:385–399

Birch DS, Morgan P, Kolden CA, Abatzoglou JT, Dillon GK, Hudak AT, Smith AM (2015) Vegetation, topography and daily weather influenced burn severity in central Idaho and western Montana forests. Ecosphere 6:1–23

Bischl B, Lang M, Kotthoff L, Schiffner J, Richter J, Studerus E, Casalicchio G, Jones ZM (2016) mlr: machine Learning in R. J Mach Learn Res 17:1–5

Blach-Overgaard A, Svenning J-C, Dransfield J, Greve M, Balslev H (2010) Determinants of palm species distributions across Africa: the relative roles of climate, non-climatic environmental factors, and spatial constraints. Ecography 33:380–391

Blomdahl EM, Kolden CA, Meddens AJ, Lutz JA (2019) The importance of small fire refugia in the central Sierra Nevada, California, USA. For Ecol Manag 432:1041–1052

Boone RB, Krohn WB (2000) Partitioning sources of variation in vertebrate species richness. J Biogeogr 27:457–470

Borcard D, Legendre P (2002) All-scale spatial analysis of ecological data by means of principal coordinates of neighbour matrices. Ecol Model 153:51–68

Borcard D, Legendre P, Drapeau P (1992) Partialling out the spatial component of ecological variation. Ecology 73:1045–1055

Bradstock RA (2009) Effects of large fires on biodiversity in south-eastern Australia: disaster or template for diversity? Int J Wildland Fire 17:809–822

Bradstock RA, Hammill KA, Collins L, Price O (2010) Effects of weather, fuel and terrain on fire severity in topographically diverse landscapes of south-eastern Australia. Landsc Ecol 25:607–619

Bucini G, Saatchi S, Hanan N, Boone RB, Smit I (2009) Woody cover and heterogeneity in the Savannas of the Kruger National Park, South Africa. In: 2009 IEEE International Geoscience and Remote Sensing Symposium. p IV–334

Camp A, Oliver C, Hessburg P, Everett R (1997) Predicting late-successional fire refugia pre-dating European settlement in the Wenatchee Mountains. For Ecol Manag 95:63–77

Cansler CA, McKenzie D (2014) Climate, fire size, and biophysical setting control fire severity and spatial pattern in the northern Cascade Range, USA. Ecol Appl 24:1037–1056

Cardador L, Sardà-Palomera F, Carrete M, Mañosa S (2014) Incorporating spatial constraints in different periods of the annual cycle improves species distribution model performance for a highly mobile bird species. Divers Distrib 20:515–528

Chen Y (2015) Distinguishing niche and neutral processes: issues in variation partitioning statistical methods and further perspectives. Comput Ecol Softw 5:130

Coen JL, Stavros EN, Fites-Kaufman JA (2018) Deconstructing the King megafire. Ecol Appl 28:1565–1580

Collins BM, Everett RG, Stephens SL (2011) Impacts of fire exclusion and recent managed fire on forest structure in old growth Sierra Nevada mixed-conifer forests. Ecosphere 2:1–14

Collins BM, Fry DL, Lydersen JM, Everett R, Stephens SL (2017a) Impacts of different land management histories on forest change. Ecol Appl 27:2475–2486

Collins BM, Miller JD, Thode AE, Kelly M, Van Wagtendonk JW, Stephens SL (2009) Interactions among wildland fires in a long-established Sierra Nevada natural fire area. Ecosystems 12:114–128

Collins BM, Stevens JT, Miller JD, Stephens, SL, Brown PM, North MP (2017b) Alternative characterization of forest fire regimes: incorporating spatial patterns. Landsc Ecol 32:1543–1552

Coppoletta M, Merriam KE, Collins BM (2016) Post-fire vegetation and fuel development influences fire severity patterns in reburns. Ecol Appl 26:686–699

Crase B, Liedloff AC, Wintle BA (2012) A new method for dealing with residual spatial autocorrelation in species distribution models. Ecography 35:879–888

Cui W, Perera AH (2008) What do we know about forest fire size distribution, and why is this knowledge useful for forest management? Int J Wildland Fire 17:234–244

Cutler DR, Edwards TC Jr, Beard KH, Cutler A, Hess KT, Gibson J, Lawler JJ (2007) Random forests for classification in ecology. Ecology 88:2783–2792

De Marco Jr P, Diniz-Filho JAF, Bini LM (2008) Spatial analysis improves species distribution modelling during range expansion. Biol Lett 4:577–580

Dennison PE, Brewer SC, Arnold JD, Moritz MA (2014) Large wildfire trends in the western United States, 1984–2011. Geophys Res Lett 41:2928–2933

Dormann CF, McPherson JM, Araújo MB, Bivand R, Bolliger J, Carl G, Davies RG, Hirzel A, Jetz W, Kissling WD, Kühn I (2007) Methods to account for spatial autocorrelation in the analysis of species distributional data: a review. Ecography 30:609–628

Dray S, Legendre P, Peres-Neto PR (2006) Spatial modelling: a comprehensive framework for principal coordinate analysis of neighbour matrices (PCNM). Ecol Model 196:483–493

Eidenshink J, Schwind B, Brewer K, Zhu ZL, Quayle B, Howard S (2007) A project for monitoring trends in burn severity. Fire Ecol 3(1):3–21

Elith J, Graham CH, Anderson RP, Dudík M, Ferrier S, Guisan A, Hijmans RJ, Huettmann F, Leathwick JR, Lehmann A, Li J (2006) Novel methods improve prediction of species' distributions from occurrence data. Ecography 29:129–151

Estes BL, Knapp EE, Skinner CN, Miller JD, Preisler HK (2017) Factors influencing fire severity under moderate burning conditions in the Klamath Mountains, northern California, USA. Ecosphere 8:e01794

Fang L, Yang J, Zu J, Li G, Zhang J (2015) Quantifying influences and relative importance of fire weather, topography, and vegetation on fire size and fire severity in a Chinese boreal forest landscape. For Ecol Manag 356:2–12

Feld CK, Birk S, Eme D, Gerisch M, Hering D, Kernan M, Maileht K, Mischke U, Ott I, Pletterbauer F, Poikane S (2016) Disentangling the effects of land use and geo-climatic factors on diversity in European freshwater ecosystems. Ecol Indic 60:71–83

Finney MA (2001) Design of regular landscape fuel treatment patterns for modifying fire growth and behavior. For Sci 47:219–228

Flint LE, Flint AL, Thorne JH, Boynton R (2013) Fine-scale hydrologic modeling for regional landscape applications: the California Basin Characterization Model development and performance. Ecol Process 2:25

Funk C, Hoell A, Stone D (2014) Examining the contribution of the observed global warming trend to the California droughts of 2012/13 and 2013/14. Bull Am Meteorol Soc 95:S11

Gesch D, Oimoen M, Greenlee S, Nelson C, Steuck M, Tyler D (2002) The national elevation dataset. Photogramm Eng Remote Sens 68:5–32

Griffin D, Anchukaitis KJ (2014) How unusual is the 2012–2014 California drought? Geophys Res Lett 41:9017–9023

Hammill KA, Bradstock RA (2009) Spatial patterns of fire behaviour in relation to weather, terrain and vegetation. Proc R Soc Qld 115:129

Harris L, Taylor AH (2015) Topography, fuels, and fire exclusion drive fire severity of the Rim Fire in an old-growth mixed-conifer forest, Yosemite National Park, USA. Ecosystems 18:1192–1208

Harris L, Taylor AH (2017) Previous burns and topography limit and reinforce fire severity in a large wildfire. Ecosphere 8(11):e02019

Hawkins BA, Diniz-Filho JAF, Mauricio BL, De Marco P, Blackburn TM (2007) Red herrings revisited: spatial autocorrelation and parameter estimation in geographical ecology. Ecography 30:375–384

Hernández-Stefanoni JL, Dupuy JM, Tun-Dzul F, May-Pat F (2011) Influence of landscape structure and stand age on species density and biomass of a tropical dry forest across spatial scales. Landsc Ecol 26:355–370

Hessburg PF, Agee JK (2003) An environmental narrative of Inland Northwest United States forests, 1800–2000. For Ecol Manag 178:23–59

Hessburg PF, Agee JK, Franklin JF (2005) Dry forests and wildland fires of the inland Northwest USA: contrasting the landscape ecology of the pre-settlement and modern eras. For Ecol Manag 211:117–139

Hessburg PF, Miller CL, Parks SA, Povak NA, Taylor AH, Higuera PE, Prichard SJ, North MP, Collins BM, Hurteau MD, Larson AJ, Allen CD, Stephens SL, Rivera-Huerta H, Stevens-Rumann CS, Daniels LD, Gedalof Z, Gray RW, Kane VR, Churchill DJ, Hagmann RK, Spies TA, Cansler CA, Belote RT, Veblen TT, Battaglia MA, Hoffman C, Skinner CN, Safford HD, Salter RB (2019) Climate, environment, and disturbance history govern resilience of Western North American Forests. Front Ecol Evol 7:239

Heyerdahl EK, Brubaker LB, Agee JK (2001) Spatial controls of historical fire regimes: a multiscale example from the interior West, USA. Ecology 82(3):660–678

Holden ZA, Morgan P, Evans JS (2009) A predictive model of burn severity based on 20-year satellite-inferred burn severity data in a large southwestern US wilderness area. For Ecol Manag 258:2399–2406

Huang J, Frimpong EA (2015) Using historical atlas data to develop high-resolution distribution models of freshwater fishes. PLoS ONE 10:e0129995

Johnson M, Crook S, Stuart M, Romero M (2013) Rim fire—preliminary fuel treatment effectiveness report. USDA For Serv Rep

Kane VR, Cansler CA, Povak NA, Kane JT, McGaughey RJ, Lutz JA, Churchill DJ, North MP (2015a) Mixed severity fire effects within the Rim fire: relative importance of local climate, fire weather, topography, and forest structure. For Ecol Manag 358:62–79

Kane VR, Lutz JA, Cansler CA, Povak NA, Churchill DJ, Smith DF, Kane JT, North MP (2015b) Water balance and topography predict fire and forest structure patterns. For Ecol Manag 338:1–13

Keane RE, Agee JK, Fulé P, Keeley JE, Key C, Kitchen SG, Miller R, Schulte LA (2009) Ecological effects of large fires on US landscapes: benefit or catastrophe? A. Int J Wildland Fire 17:696–712

Keeley JE, Syphard AD (2019) Twenty-first century California, USA, wildfires: fuel-dominated vs. wind-dominated fires. Fire Ecol 15(1):24

Key CH, Benson NC (2006) Landscape assessment (LA). FIREMON: fire effects monitoring and inventory system. Gen Tech Rep RMRS-GTR-164-CD 1:164

Komac B, Esteban P, Trapero L, Caritg R (2016) Modelization of the current and future habitat suitability of *Rhododendron ferrugineum* using potential snow accumulation. PLoS ONE 11:e0147324

LANDFIRE (2012) Existing vegetation type layer, LANDFIRE 1.3.0

Lareau NP, Nauslar NJ, Abatzoglou JT (2018) The Carr Fire Vortex: a case of Pyrotornadogenesis? Geophys Res Lett 45(23):13–107

Legendre P (1993) Spatial autocorrelation: trouble or new paradigm? Ecology 74:1659–1673

Lemm JU, Feld CK, Birk S (2019) Diagnosing the causes of river deterioration using stressor-specific metrics. Sci Total Environ 651:1105–1113

Lentile LB, Smith FW, Shepperd WD (2006) Influence of topography and forest structure on patterns of mixed severity fire in ponderosa pine forests of the South Dakota Black Hills, USA. Int J Wildland Fire 15:557–566

Lundquist JD, Pepin N, Rochford C (2008) Automated algorithm for mapping regions of cold-air pooling in complex terrain. J Geophys Res Atmos. https://doi.org/10.1029/2008JD009879

Lutz JA, Key CH, Kolden CA, Kane JT, van Wagtendonk JW (2011) Fire frequency, area burned, and severity: a quantitative approach to defining a normal fire year. Fire Ecol 7:51–65

Lydersen JM, Collins BM (2018) Change in vegetation patterns over a large forested landscape based on historical and contemporary aerial photography. Ecosystems. https://doi.org/10.1007/s10021-018-0225-5

Lydersen JM, Collins BM, Brooks ML, Matchett JR, Shive KL, Povak NA, Kane VR and Smith DF (2017) Evidence of fuels management and fire weather influencing fire severity in an extreme fire event. Ecol Appl 27:2013–2030

Lydersen JM, Collins BM, Miller JD, Fry DL, Stephens SL (2016) Relating fire-caused change in forest structure to remotely sensed estimates of fire severity. Fire Ecol 12:99–116

Lydersen J, North M (2012) Topographic variation in structure of mixed-conifer forests under an active-fire regime. Ecosystems 15:1134–1146

Lydersen JM, North MP, Collins BM (2014) Severity of an uncharacteristically large wildfire, the Rim Fire, in forests with relatively restored frequent fire regimes. For Ecol Manag 328:326–334

Mallek C, Safford H, Viers J, Miller J (2013) Modern departures in fire severity and area vary by forest type, Sierra Nevada and southern Cascades, California, USA. Ecosphere 4:1–28

Martinez AJ, Meddens AJ, Kolden CA, Strand EK, Hudak AT (2019) Characterizing persistent unburned islands within the Inland Northwest USA. Fire Ecol 15:20

Mascaro J, Asner GP, Knapp DE, Kennedy-Bowdoin T, Martin RE, Anderson C, Higgins M, Chadwick KD (2014) A tale of two "forests": random forest machine learning aids tropical forest carbon mapping. PLoS ONE 9:e85993

Meddens AJ, Kolden CA, Lutz JA, Smith AM, Cansler CA, Abatzoglou JT, Meigs GW, Downing WM, Krawchuk MA (2018) Fire refugia: what are they, and why do they matter for global change? BioScience 68(12):944–954

Meyer MD (2015) Forest fire severity patterns of resource objective wildfires in the southern Sierra Nevada. J For 113:49–56

Miller JD, Collins BM, Lutz JA, Stephens SL, van Wagtendonk JW, Yasuda DA (2012) Differences in wildfires among ecoregions and land management agencies in the Sierra Nevada region, California, USA. Ecosphere 3(9):1–20

Miller JD, Knapp EE, Key CH, Skinner CN, Isbell CJ, Creasy RM, Sherlock JW (2009) Calibration and validation of the relative differenced Normalized Burn Ratio (RdNBR) to three measures of fire severity in the Sierra Nevada and Klamath Mountains, California, USA. Remote Sens Environ 113:645–656

Miller JD, Quayle B (2015) Calibration and validation of immediate post-fire satellite-derived data to three severity metrics. Fire Ecol 11(2):12–30

Miller JD, Safford H (2012) Trends in wildfire severity: 1984 to 2010 in the Sierra Nevada, Modoc Plateau, and southern Cascades, California, USA. Fire Ecol 8:41–57

Miller JD, Thode AE (2007) Quantifying burn severity in a heterogeneous landscape with a relative version of the delta Normalized Burn Ratio (dNBR). Remote Sens Environ 109:66–80

Minder JR, Mote PW, Lundquist JD (2010) Surface temperature lapse rates over complex terrain: lessons from the Cascade Mountains. J Geophys Res. https://doi.org/10.1029/2009JD013493

O'Connor CD, Calkin DE, Thompson MP (2017) An empirical machine learning method for predicting potential fire control locations for pre-fire planning and operational fire management. Int J Wildland Fire 26:587–597

Odion DC, Frost EJ, Strittholt JR, Jiang H, Dellasala DA, Moritz MA (2004) Patterns of fire severity and forest conditions in the western Klamath Mountains, California. Conserv Biol 18:927–936

Oksanen J, Blanchet FG, Friendly M, Kindt R, Legendre P, McGlinn D, Minchin PR, O'Hara RB, Simpson GL, Solymos P, Stevens MH, Szoecs E, Wagner H (2018) vegan: Community Ecology Package. R package version 2.5-4. https://CRAN.R-project.org/package=vegan

Olden JD, Lawler JJ, Poff NL (2008) Machine learning methods without tears: a primer for ecologists. Q Rev Biol 83:171–193

Parks S, Dobrowski S, Panunto M (2018a) What drives low-severity fire in the Southwestern USA? Forests 9:165

Parks SA, Holsinger LM, Panunto MH, Jolly WM, Dobrowski SZ, Dillon GK (2018b) High-severity fire: evaluating its key drivers and mapping its probability across western US forests. Environ Res Lett 13:044037

Parks SA, Miller C, Nelson CR, Holden ZA (2014) Previous fires moderate burn severity of subsequent wildland fires in two large western US wilderness areas. Ecosystems 17:29–42

Parks SA, Parisien M-A, Miller C (2011) Multi-scale evaluation of the environmental controls on burn probability in a southern Sierra Nevada landscape. Int J Wildland Fire 20:815–828

Peterson D, Campbell J, Hyer E, Fromm M, Kablick G, Cossuth J, DeLand M (2018) Wildfire-driven thunderstorms cause a volcano-like stratospheric injection of smoke. Clim Atmos Sci 1:30

Peterson DA, Hyer EJ, Campbell JR, Fromm MD, Hair JW, Butler CF, Fenn MA (2015) The 2013 rim fire: implications for predicting extreme fire spread, pyroconvection, and smoke emissions. Bull Am Meteorol Soc 96:229–247

Portier J, Gauthier S, Robitaille A, Bergeron Y (2018) Accounting for spatial autocorrelation improves the estimation of climate, physical environment and vegetation's effects on boreal forest's burn rates. Landsc Ecol 33:19–34

Povak NA, Hessburg PF, Salter RB (2018) Evidence for scale-dependent topographic controls on wildfire spread. Ecosphere 9:e02443

Prichard SJ, Kennedy MC (2014) Fuel treatments and landform modify landscape patterns of burn severity in an extreme fire event. Ecol Appl 24:571–590

Prichard SJ, Stevens-Rumann CS, Hessburg PF (2017) Tamm Review: shifting global fire regimes: Lessons from reburns and research needs. For Ecol Manag 396:217–233

PRISM Climate Group (2013) PRISM Climate Data. Or State Univ http://prism.oregonstate.edu, Created 10 July 2012:

R Core Team (2018) R: a language and environment for statistical computing. R Foundation for Statistical Computing, Vienna

Qiu Y, Mei J (2018) RSpectra: Solvers for Large-Scale Eigenvalue and SVD Problems

Quisthoudt K, Adams J, Rajkaran A, Dahdouh-Guebas F, Koedam N, Randin CF (2013) Disentangling the effects of global climate and regional land-use change on the current and future distribution of mangroves in South Africa. Biodivers Conserv 22:1369–1390

Reshetnikov AN, Ficetola GF (2011) Potential range of the invasive fish rotan (*Perccottus glenii*) in the Holarctic. Biol Invasions 13:2967–2980

Rollins MG, Morgan P, Swetnam T (2002) Landscape-scale controls over twentieth century fire occurrence in two large Rocky Mountain (USA) wilderness areas. Landsc Ecol 17:539–557

Ryo M, Yoshimura C, Iwasaki Y (2018) Importance of antecedent environmental conditions in modeling species distributions. Ecography 41:825–836

Safford HD, Stevens J, Merriam K, Meyer MD, Latimer AM (2012) Fuel treatment effectiveness in California yellow pine and mixed conifer forests. For Ecol Manag 274:17–28

Scholl AE, Taylor AH (2010) Fire regimes, forest change, and self-organization in an old-growth mixed-conifer forest, Yosemite National Park, USA. Ecol Appl 20:362–380

Singleton MP, Thode AE, Meador AJS, Iniguez JM (2019) Increasing trends in high-severity fire in the southwestern USA from 1984 to 2015. For Ecol Manag 433:709–719

Stavros EN, Abatzoglou JT, McKenzie D, Larkin NK (2014) Regional projections of the likelihood of very large wildland fires under a changing climate in the contiguous Western United States. Clim Change 126:455–468

Steel ZL, Koontz MJ, Safford HD (2018) The changing landscape of wildfire: burn pattern trends and implications for California's yellow pine and mixed conifer forests. Landsc Ecol 33:1159–1176

Stephens SL, Burrows N, Buyantuyev A, Gray RW, Keane RE, Kubian R, Liu S, Seijo F, Shu L, Tolhurst KG, van Wagtendonk JW (2014) Temperate and boreal forest megafires: characteristics and challenges. Front Ecol Environ 12:115–122

Stevens JT, Collins BM, Miller JD, North MP, Stephens SL (2017) Changing spatial patterns of stand-replacing fire in California conifer forests. For Ecol Manag 406:28–36

Stevens-Rumann CS, Prichard SJ, Strand EK, Morgan P (2016) Prior wildfires influence burn severity of subsequent large fires. Can J For Res 46:1375–1385

Strobl C, Boulesteix A-L, Kneib T, Augustin T, Zeileis A (2008) Conditional variable importance for random forests. BMC Bioinform 9:307

Strobl C, Boulesteix AL, Zeileis A, Hothorn T (2007) Bias in random forest variable importance measures: illustrations, sources and a solution. BMC Bioinform 8(1):25

Thompson JR, Spies TA (2009) Vegetation and weather explain variation in crown damage within a large mixed-severity wildfire. For Ecol Manag 258:1684–1694

Václavík T, Kupfer JA, Meentemeyer RK (2012) Accounting for multi-scale spatial autocorrelation improves performance of invasive species distribution modelling (iSDM). J Biogeogr 39:42–55

Van de Water K, North M (2010) Fire history of coniferous riparian forests in the Sierra Nevada. For Ecol Manag 260(3):384–395

van Wagtendonk JW (2007) The history and evolution of wildland fire use. Fire Ecol 3(2):3–17

van Wagtendonk K (2012) Fires in previously burned areas: fire severity and vegetation interactions in Yosemite National Park. 2011 George Wright Society Biennial Conference on Parks, Protected Areas, and Cultural Sites. George Wright Society, Hancock, pp 356–363

van Wagtendonk JW, van Wagtendonk KA, Thode AE (2012) Factors associated with the severity of intersecting fires in Yosemite National Park, California, USA. Fire Ecol 8:11–31

Werth PA, Potter BE, Alexander ME, Clements CB, Cruz MG, Finney MA, Forthofer JM, Goodrick SL, Hoffman C, Jolly WM, McAllister SS, Ottmar RD, Parsons RA (2016) Synthesis of knowledge of extreme fire behavior: volume 2 for fire behavior specialists, researchers, and meteorologists. Gen Tech Rep PNW-GTR-891 Portland US Dep Agric For Serv Pac Northwest Res Stn 258 P 891

Westerling AL (2016) Increasing western US forest wildfire activity: sensitivity to changes in the timing of spring. Phil Trans R Soc B 371:20150178

Williams AP, Seager R, Abatzoglou JT, Cook BI, Smerdon JE, Cook ER (2015) Contribution of anthropogenic warming to California drought during 2012–2014. Geophys Res Lett 42:6819–6828

Wimberly MC, Cochrane MA, Baer AD, Pabst K (2009) Assessing fuel treatment effectiveness using satellite imagery and spatial statistics. Ecol Appl 19:1377–1384

Publisher's Note Springer Nature remains neutral with regard to jurisdictional claims in published maps and institutional affiliations.